SSC-183

Metallurgical Structure and the Brittle Behavior of Steel

by

MORRIS COHEN

SHIP STRUCTURE COMMITTEE

SHIP STRUCTURE COMMITTEE

MEMBER AGENCIES:
UNITED STATES COAST GUARD
NAVAL SHIP SYSTEMS COMMAND
MILITARY SEA TRANSPORTATION SERVICE
MARITIME ADMINISTRATION
AMERICAN BUREAU OF SHIPPING

ADDRESS CORRESPONDENCE TO:
SECRETARY
SHIP STRUCTURE COMMITTEE
U.S. COAST GUARD HEADQUARTERS
WASHINGTON, D.C. 20591

May 1968

Dear Sir:

The Ship Structure Committee sponsored a long-term study at Massachusetts Institute of Technology to study the influence of metallurgical structure on the fracture behavior of ship steel. The accomplishments of this project are described in the enclosed final report, *Metallurgical Structure and the Brittle Behavior of Steel* by Morris Cohen.

This project is being conducted under the advisory guidance of the Ship Hull Research Committee of the National Academy of Sciences-National Research Council.

This report is being distributed to individuals and groups associated with or interested in the work of the Ship Structure Committee. Comments concerning this report are solicited.

Sincerely yours,

D. B. Henderson
Rear Admiral U. S. Coast Guard
Chairman, Ship Structure
Committee

SSC - 183

Final Report
of
Project SR - 136
"Metallurgical Structure"

to the
Ship Structure Committee

METALLURGICAL STRUCTURE AND THE BRITTLE BEHAVIOR OF STEEL

by

Morris Cohen

Massachusetts Institute of Technology

under
Department of the Navy
Naval Ship Systems Command
Contract NObs - 88279

May 1968

ABSTRACT

This report provides a coherent summary of a long-range research program on the metallurgical factors that govern the brittle behavior of mild steels and the relevant micromechanisms of fracture. For much of the experimental procedures and findings, attention is drawn to the reports and papers stemming from this investigation, listed at the end of the present report. Somewhat more emphasis is placed herein on the later phases of the program which have not been published yet.

By means of surface-replication and three-dimensional metallography, it has become possible to delineate the interrelated processes of slip, twinning, carbide cracking void formation and microcleavage in the tensile testing of iron and mild steels at subatmospheric temperatures. Under these conditions, the ductility-transition temperature (T_d) is defined as the temperature below which fracture takes place prior to the necking instability. Hence, below T_d, the ductility is low but not necessarily zero.

Carbides undergo cracking during plastic straining, and furnish sites either for microcleavage initiation (if the Griffith-Orowan condition is satisfied when the carbide crack comes into existence) or for void formation. These are competitive processes, with full cleavage fracture predominating in the vicinity of T_d. Descriptions are given of the processes by which voids link up via localized necking and by which microcleavages propagate across grain boundaries or link up with each other.

Mechanical twinning plays a complex but secondary role in these polycrystalline materials. At temperatures well below T_d, twinning supersedes slip as the primary mode of deformation, and the collision of a moving twin with an existing one becomes an active source of microcleavage, thus leading to further reduction in ductility. These twinning phenomena become more evident with increasing grain size and increasing yield strength. On the other hand, preexisting twins can act as barriers to the propagation of cleavage fracture, thereby leading to a lowering of T_d and enhanced ductility. Furthermore, in some instances, the twin interfaces are mobile and contribute additional modes of local plasticity that tend to relieve the acting microstresses; this inhibits the initiation of microcleavage. These beneficial effects of preexisting twins are quite pronounced in tensile tests, but they are less advantageous in Charpy testing.

The cracking of intergranular carbides is an especially potent means of microcleavage initiation, and can be used as a "tell-tale" to follow the fracturing sequences. This approach has been adopted to study the influence of notches in tensile testing and in slow-bend testing.

In certain ranges of temperature, double yield points are observed in the notched tensile tests because of the first yielding in the notched volume and the subsequent yielding in the outer volume. In both types of notched specimens, fibrous fracture starts at the notch root due to void formation, whereas cleavage fracture starts about one millimeter away from the root due to preferential microcleavage there.

There are indications that the amount and size of intergranular carbides in mild steels are reduced by decreased carbon content, increased manganese content, increased cooling rate from the austenitizing temperature, and decreased grain size; this could account, at least in part, for the favorable effects of such changes on the fracture behavior.

The initiation of microcleavage via carbide cracking can be treated statistically, on the assumption that the number of carbide cracks per unit volume is proportional to the plastic strain, and that the size distribution of carbide cracks at any given strain is parobolic up to the maximum size present. A graphical calculation can then be made of the number of microcleavages generated at each point along the stress-strain curve, based on the number of carbide cracks (being produced at the given strain) having lengths that are supercritical (in the Griffith–Orowan sense) at the given stress. Any carbide crack forming that happens to be subcritical at the time becomes blunted and is taken to remain inert relative to microcleavage at subsequently higher stresses. These considerations lead to calculations of the correct form for the number of microcleavages observed in tensile-tested specimens at various temperatures, and also for the ductility-transition temperature as influenced by several metallurgical variables.

An important step remains to connect up these microfracturing processes with macrocrack formation in plate sections.

CONTENTS

		Page
1.	Introduction	1
2.	Evaluation of Brittle Fracture from a Research Standpoint	1
3.	Microcleavage Phenomena	3
4.	Types of Ship Steels Investigated	4
5.	Grain Size	4
6.	Cooling Rate as a Factor	4
7.	Role of Carbides in Initiating Fracture	5
8.	Cleavage Fracture in Iron Single Crystals	8
9.	Twinning as a Means of Structural Refinement	10
10.	Micromechanisms of Fracture in the Presence of Notches	10
	Notched-Tensile Tests	10
	Notched-Bend Tests	14
11.	Statistical Nature of Cleavage Initiation	17
12.	Macrocrack Formation	20
	Acknowledgments	23
	References	23

SHIP STRUCTURE COMMITTEE

The SHIP STRUCTURE COMMITTEE is constituted to prosecute a research program to improve the hull structures of ships by an extension of knowledge pertaining to design, materials and methods of fabrication.

RADM D. B. Henderson, USCG - Chairman
Chief, Office of Engineering
U. S. Coast Guard Headquarters

Captain R. T. Miller, USN
Head, Ship Engineering Department
Naval Ship Engineering Center

Captain T. J. Banvard, USN
Maintenance and Repair Officer
Military Sea Transportation Service

Mr. E. Scott Dillon
Chief, Division of Ship Design
Office of Ship Construction
Maritime Administration

Mr. D. B. Bannerman, Jr.
Vice President - Technical
American Bureau of Shipping

SHIP STRUCTURE SUBCOMMITTEE

The SHIP STRUCTURE SUBCOMMITTEE acts for the Ship Structure Committee on technical matters by providing technical coordination for the determination of goals and objectives of the program, and by evaluating and interpreting the results in terms of ship structural design, construction and operation.

NAVAL SHIP ENGINEERING CENTER

Mr. J. J. Nachtsheim - Chairman
Mr. John Vasta - Contract Administrator
Mr. George Sorkin - Member
Mr. Ivo Fioriti - Alternate

MARITIME ADMINISTRATION

Mr. R. W. Black - Member
Mr. Anatole Maillar - Member
Mr. R. Falls - Alternate
Mr. W. G. Frederick - Alternate

AMERICAN BUREAU OF SHIPPING

Mr. G. F. Casey - Member
Mr. F. J. Crum - Member

OFFICE OF NAVAL RESEARCH

Mr. J. M. Crowley - Member
Dr. Wm. G. Rauch - Alternate

MILITARY SEA TRANSPORTATION SERVICE

LCDR Donald B. Bosley, USN - Member
Mr. R. R. Askren - Member

U. S. COAST GUARD

CDR C. R. Thompson, USCG - Member
Mr. J. B. Robertson, Jr. - Member
LCDR James L. Howard, USCG - Alternate
LCDR R. Nielsen, Jr., USCG - Alternate

NAVAL SHIP RESEARCH & DEVELOPMENT CENTER

Mr. A. B. Stavovy - Alternate

LIAISON REPRESENTATIVES

NATIONAL ACADEMY OF SCIENCES-
NATIONAL RESEARCH COUNCIL

Mr. A. R. Lytle - Director, Ship Research Committee
Mr. R. W. Rumke - Executive Secretary, SRC

AMERICAN IRON AND STEEL INSTITUTE

Mr. J. R. LeCron

BRITISH NAVY STAFF

Mr. A. C. Law
Construction CDR T. R. Rumens, RCNC

WELDING RESEARCH COUNCIL

Mr. K. K. Koopman, Director
Mr. Charles Larson, Asst. Director

1. Introduction

This report presents a summary of long-range research on the brittle fracture of mild steels, undertaken at M.I.T. under the technical cognizance of the then Committee on Ship Steel and now the Ship Hull Research Committee. The program started in June 1954 and terminated in December 1966, having been initiated as a result of the 1953 Barrett-Mahin report[1], which pointed up a critical need for establishing the fundamental role of metallurgical structure in the brittle behavior of steel, with special emphasis on the micromechanisms at play. The program was supervised at M.I.T. by Professors Morris Cohen and B. L. Averbach throughout the ensuing period.

Aside from the technical findings to be reviewed here, it is worth noting that this project provided an important focus on the subject of brittle fracture around the world and, through advanced-degree theses as well as post-doctoral research, evolved a significant group of investigators, many of whom have remained active in the field after leaving M.I.T. They are listed below in chronological order:

Donald H. Whitmore
Walter S. Owen
C. Patrick Sullivan
Ronald S. Kintisch
Walter R. Johnson
William F. Flanagan
George T. Hahn
Ryukichi Honda
Barry H. Rosof
Charles J. McMahon, Jr.
Mikael Grounes
Phillipe Delori
Henry J. Rack
Milan R. Vukcevich
Takashi Furukawa

This research program also led to an International Conference on Fracture in Swampscott, Massachusetts in 1959[2], and thereby to another International Conference on Fracture in Sendai, Japan in 1965[3]. The latter meeting gave impetus to the new International Journal on Fracture Mechanics in 1965. In addition, over the years a substantial portion of the American participation on the fundamentals of brittle fracture at the annual meetings of the International Institute of Welding was contributed by the M.I.T. group. On one such occasion, the 1961 Eduard Houdrement Lecture was given by Morris Cohen on "Metallurgical Factors in the Low-Temperature Behavior of Mild Steel."

The main papers and reports[4-19] arising from this project are listed according to date in the references.

2. Evaluation of Brittle Fracture from a Research Standpoint

The tests regularly used in the study of brittle fracture have been the subject of considerable argument. On the basis of data relating to ship failures, it appears that the Charpy V-notch test with a transition temperature defined by the 10 or 15 ft-lb level provides a useful and convenient criterion for comparing steels within the American Bureau of Shipping classification system. However, several other tests, such as the drop weight, the explosion bulge and the notched tensile, have been employed advantageously, particularly for steels with higher alloy contents.

For research on metallurgical structure, it is quite informative to test unnotched tensile bars at subatmospheric temperatures. Typical results are shown in Figure 1 for a steel (0.16 percent carbon, 1.0 percent manganese) which meets the current ABS Class B specification. The yield and fracture strengths rise as the test temperature is lowered. At a sufficiently low temperature, however, (-195^{o} C in this case) there is a comparatively abrupt decrease in fracture stress, which is also accompanied by a sudden decrease in ductility to some low level but *not to zero*. The temperature at which these changes occur is defined as the ductility-transition temperature (T_d) of the steel for the test conditions at hand. At still lower temperatures (say below -200^{o} C in this instance), yielding does not start by the usual slip mechanism but by the onset of mechanical twinning. It is of interest that in this range of temperatures, the twinning and fracture stresses are rather close and are evidently related. In this temperature region, the ductility decreases further and becomes extremely small.

Above T_d, the true stress at the point of plastic instability (associated with necking) rises with decreasing test temperature, following a course intermediate between the yield and fracture stresses. T_d itself is determined by the necking phenomenon; that is, at higher temperatures, necking occurs before fracture, and a large reduction of area results, whereas at lower temperatures, fracture takes place without prior necking and the reduction of area is correspondingly small.

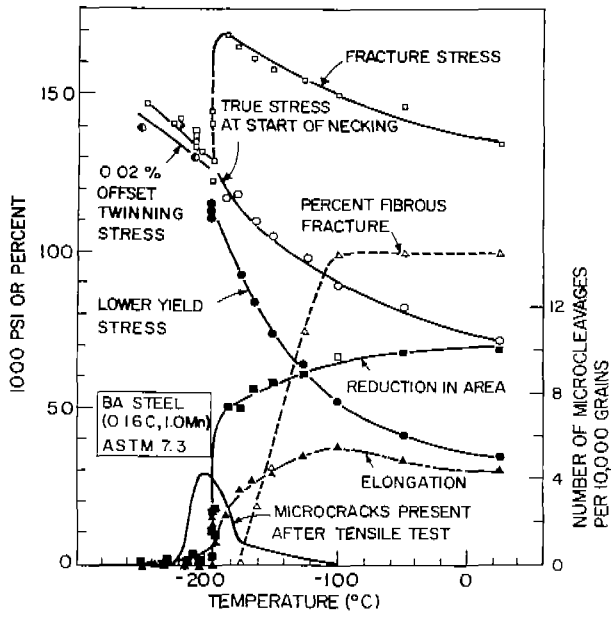

Fig. 1. Tensile Properties Vs. Test Temperature For A Mild Steel. All Specimens Homogenized At 1250° C For 24 Hours Before Subsequent Annealing At 880°C To Develop The Indicated Grain Size In The Furnace-Cooled Condition.

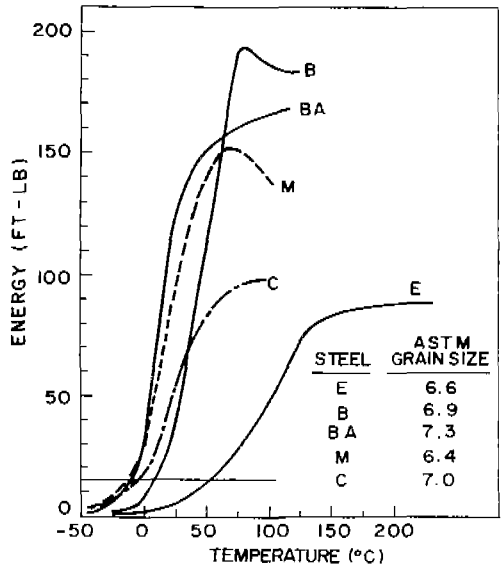

Fig. 2. Charpy V-Notch Impact Energy Of Mild Steels As A Function Of Test Temperature. All Specimens Homogenized For 24 Hours At 1250°C Before Subsequent Annealing To Develop The Indicated Grain Size In The Furnace-Cooled Condition.

TABLE. 1. TRANSITION TEMPERATURES OF SHIP STEELS.

Steel	Composition w/o C	w/o Mn	w/o Si	Deoxidation Practice	ASTM Grain Size	Transition Temperature (°C) Tensile (T_d)	Charpy V-15 ft-lb.
E	0.22	0.36	0.002	rimmed	6.6	-156	52
B	0.16	0.69	0.022	semikilled	6.9	-182	8
BA	0.18	1.0	0.046	semikilled	7.3	-195	- 9
M	0.16	1.3	0.024	semikilled	6.4	-195	-13
C	0.20	0.62	0.19	killed	7.0	-195	- 4

All steels homogenized at 1250° C for 24 hours, then austenitized at temperatures between 870 - 900° C and furnace-cooled to produce equiaxed ferrite and pearlite.

By the same token, T_d does not coincide with the entree of cleavage fracture. According to Figure 1, fracture occurs by cleavage to an increasing extent as the test temperature drops below about -100° C (cf. curve marked "percent fibrous fracture") and becomes completely cleavage at -187°C. Thus, between this temperature and the ductility-transition temperature of -195° C, necking and large reductions of area take place before fracture, and yet the fracture is fully cleavage. Below T_d, the fracture is still completely cleavage, but there the ductility is small because fracture sets in without any prior necking. There are many instances, however, in which the ductility-transition temperature does occur just as the fracture becomes fully cleavage.

Microcleavage cracks in the ferritic grains are detected on tensile testing below -100° C, and these cracks become more frequent with decreasing test temperature, particularly in the range near T_d. However, the number of microcleavages reaches a maximum, and then goes to substantially zero at still lower temperatures. It is evident that, over the temperature range spanned by the bell-shaped microcleavage-frequency curve, these small cracks are being arrested short of complete propagation to failure, and that the conditions for cleavage initiation are not the same as for complete cleavage fracture. Moreover in view of the fact that microcleavages can be found in specimens that ultimately fail by full cleavage fracture, this means that the microcracks, once arrested, are resistant to further propagation even at higher stresses than those attending their initiation.

In the illustrative steel under discussion, the primary mode of plastic deformation preceding cleavage fracture switches from slip to twinning as the test temperature drops below T_d. This circumstance offers a reason why cleavage occurs without prior necking at temperatures below T_d. Thus, deformation by twinning has a tendency to promote brittle fracture and can be a deleterious phenomenon from that standpoint. Nevertheless, there are cases in which twinning enters a primary mode of deformation only at temperatures well below T_d. Consequently, twinning is not a necessary condition for the existence of the ductility-transition phenomenon.

The Charpy V-notch curves for a number of low-carbon steels are shown in Figure 2. These steels (Table I) were homogenized for 24 hours at 1250° C and were then treated to produce a uniform grain size, about ASTM 7, in the furnace-cooled condition. Although there is much detail in these curves, attention is focussed on the 15 ft-lb transition temperatures which usually rate the steels according to their propensity to undergo brittle fracture in service. These transition temperatures together with the ductility-transition temperatures exhibited by the smooth-bar tensile tests are summarized in Table I. Both tests, although widely different in character, rank the steels in approximately the same order. However, because of the different mechanical factors embodied in these tests, we have found it appropriate to use both Charpy (slow-bend as well as impact) and tensile data in this research. For example, the 15 ft-lb transition temperatures show a larger spread among the various steels than do the tensile ductility-transition temperatures, but both decrease equally with decreasing ferritic grain size, being of the order of 10° C per ASTM number.

3. Microcleavage Phenomena

Cleavage microcracks in the ferritic grains are found in tensile specimens loaded above the yield stress at temperatures above and below T_d. The fraction of grains thus cracked increased with decreasing test temperature, reaches a maximum, and drops to zero with further decrease in temperature (Figure 1). Obviously then, the conditions for initiating and propagating a cleavage crack within a grain of ferrite do not necessarily satisfy the conditions for complete fracture of the specimen. When microcracks are detected before ultimate failure, it means that the cleavage process has started and stalled on a microscale. This stopping of microcleavage propagation occurs at barriers, such as grain boundaries and pre-existing mechanical twins, and by competitive slip or twinning at the tip of the advancing crack.

There is good evidence that many microcleavages do not propagate further once they have stopped. With increasing applied stress, such cracks tend to widen because localized plastic deformation results in a blunting of the tip. It is thought that for the most part, complete cleavage takes place when a microcrack is initiated at a high enough stress (or under high enough stored energy) to keep the crack running across grain boundaries as well as grains, without being arrested by concomitant deformation just ahead of the tip. At lower testing temperatures, where no microcracks are found prior to complete cleavage fracture, the first microcrack is initiated under conditions which permit it to propagate all the way to failure. Only at such temperatures do the conditions for cleavage initiation really correspond to the fracture stress.

Although the ferrite microcleavage is always (at least in our studies) preceded by some plastic deformation, the latter process may involve either slip or twinning. Twinning is more effective than slip in this regard, but it is not an essential occurrence for the formation of microcleavage in iron and in ship steels. As will be discussed in Section 7, the early cracking of grain-boundary carbide films often plays a key role in initiating cleavage of the ferrite. The temperature range in which ferrite microcleavage is detected usually straddles the ductility-transition temperature. However, the temperature of maximum microcleavage-frequency does not necessarily coincide with T_d. Moreover, in the Steel M[12], these microcracks are rarely observed at any test temperature, suggesting that here the initiation stage is the difficult step, and once achieved, the cleavage proceeds to complete fracture. Yet, microcracking is readily noted in fairly pure iron [10, 15, 16].

4. Types of Ship Steels Investigated

The steels used in this program (Table 1) include some common grades of ABS ship steel. Steel B is an example of an old Class B steel, which was superseded in 1955 by a newer Class B (listed as BA in Table 1) with a higher manganese range and a lower maximum carbon content. Steel M is an experimental semikilled steel with a high manganese-carbon ratio. Steel C is a killed (typical of ABS Class C made with fine-grain practice), and Steel E is an unusually brittle rimmed steel (otherwise known as Project E Steel).

The data for the semikilled series (Steels B, BA and M) in Table 1 show that increasing the manganese-carbon ratio is helpful in lowering both the tensile and Charpy transition temperatures at constant ferritic grain size. Semikilled Steels BA and M have transition temperatures in the same range as the killed Steel C at comparable grain size. However, as a rule, killed steels are advantageous in that they tend to have finer grain sizes than do the semikilled steels in regular commercial practice*. Likewise, the highest-manganese Steel M may offer an advantage over the intermediate-manganese Steel BA in this respect.

*It should be noted that Steel C happens to have a higher carbon content than the three semikilled steels investigated here. At the same carbon level, Steel C would have a somewhat lower transition temperature.

5. Grain Size

It is well known that the ferritic grain size is an important parameter in brittle behavior. In fact, both the tensile and Charpy transition temperatures are sensitive to this metallurgical feature. However, in order to sort out the effect of grain size, it is necessary to avoid the formation of platelike ferrite (i.e., Widmanstätten structures) and to take into account factors arising from differences in the cooling rate from the austenitizing temperature.

Although the average grain diameter of the ferrite describes the ferritic grain size appropriately when the ferrite is equiaxed, uncertainties develop when Widmanstätten ferrite is present[5]. Inasmuch as some of the ferritic plates are almost as long as the austenitic grain diameter, it is possible that fracture paths may exist in these structures which are much longer than that corresponding to the average linear dimension of the platelike ferrite. Thus, in a Widmanstätten structure, the ferrite may behave as though it had an unexpectedly large grain size. Illustrative data are given in Figure 3[5].

In order to vary the ferritic grain size systematically in these studies, the steels were subjected to a range of annealing or normalizing temperatures. Unfortunately, such treatments also change the grain size of the parent austenite and the patch size of the pearlite. However, the ferritic grain size yields the most consistent correlation with the ductility-transition behavior. This becomes especially clear in relatively pure iron where pearlite is not present and the ferritic grain size can be controlled by cold-working and subcritical annealing. Nevertheless, in ship steels, both the pearlite and austenitic grain size may contribute, at least in a secondary manner. Microcracks can initiate in the pearlitic patches, and coarse austenitic grains are conducive to the formation of Widmanstätten structures which act to raise the transition temperature (Figure 3).

6. Cooling Rate as a Factor

It is now fairly well established that air cooling (~ 150° C per minute) from the austenitizing temperature is preferable to furnace cooling (~ 1.5° C per minute) from the standpoint of reducing the susceptibility to brittle fracture. Both rates of cooling lead to ferrite-pearlite structures, but the faster cooling results in a smaller ferritic grain size

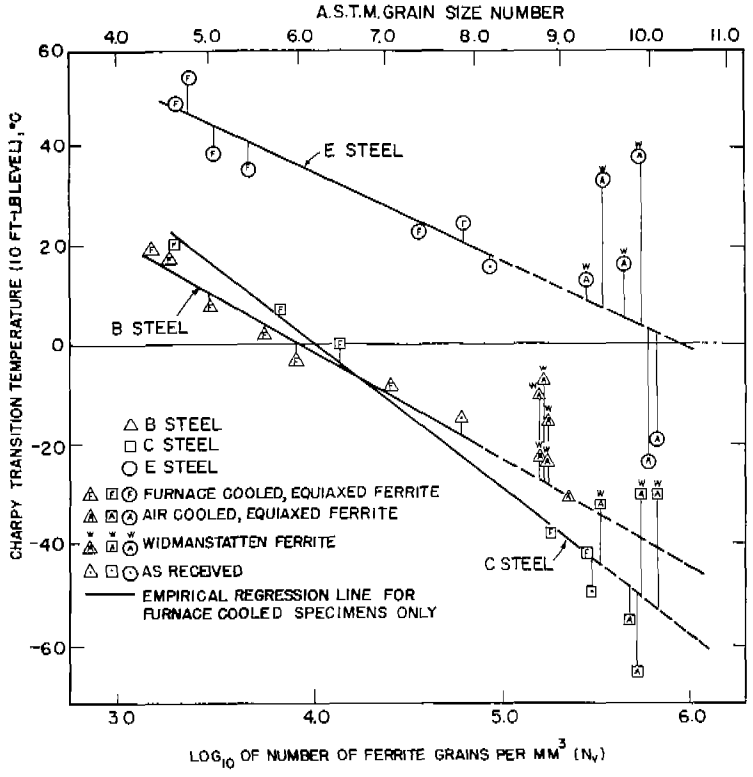

Fig. 3. Relationship between ferrite grain size and Charpy transition temperature (10 ft-lb level). Note higher transition temperatures for Widmanstätten structures at any given grain size.

despite the fact that the austenitic grain size is the same in the two cases*. However, even after correcting for differences in ferritic grain size, the transition temperature after air cooling is lower than that after furnace cooling. To test this point more directly, specimens of Steel C were heat treated to the same grain size in both the air-cooled and the furnace-cooled conditions by adopting higher austenitizing temperatures for the former treatments[5]. The Charpy 15 ft-lb transition temperature was almost 20°C lower for the air-cooled series than for the furnace-cooled series.

This effect of cooling rate is of practical importance. We have not been able to connect it up with differences in the amount of pearlite or in the substructure of the ferrite. The dislocation arrays and subgrains have shown no correlation with the observed change in tendency to brittle fracture.[13] However, the extent of carbide precipitation at the grain boundaries turns out to be an important microstructural variable in this connection, as indicated below.

7. Role of Carbides in Initiating Fracture

Pearlitic patches often crack during tensile testing at subzero temperatures; the fracture strength of the pearlite is probably related to the spacing of the lamellae and the proportion of carbide in the aggregate. However, all the steels listed in Table I had pearlite contents between 10 and 20 volume percent, whether in the furnace-cooled or air-cooled state, and no consistent trends in

* This is another instance in which the transition temperature is found to change with the ferritic grain size rather than with the austenitic grain size.

fracture behavior with respect to the amount of pearlite were observed in this limited range. Ferrite microcracking is much more prevalent than pearlite microcracking, and the role of carbides along grain boundaries appears to be more critical than that of pearlite.

There is little doubt that carbides at grain boundaries tend to be damaging. Grain-boundary carbide films crack easily and can initiate cleavage of the adjacent ferrite. We have used a technique[15,16] in which the evolution of microcracks during a tensile test can be observed by taking plastic replicas of prepolished surface after unloading from successively higher stresses. A three-mil thick strip of cellulose acetate is pressed against the surface of a specimen (Figure 4), using a film of acetone at the interface to soften the

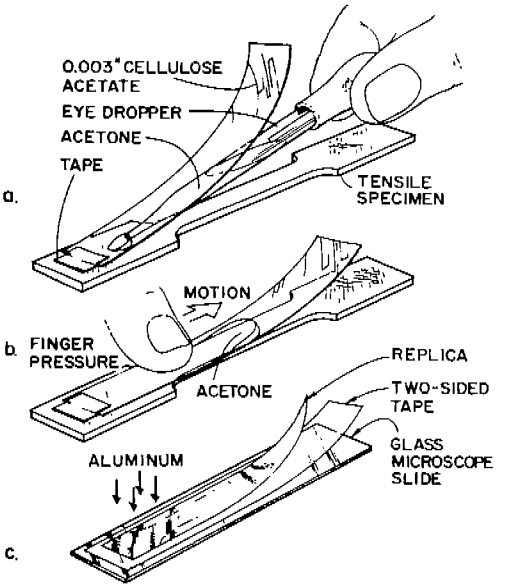

Fig. 4. Replication Technique For Recording Surface Detail.

acetate and improve the contact. The replica thus produced is peeled off the specimen and then coated with aluminum via vapor-phase deposition. The purpose of the aluminum coating is to provide high reflectivity and contrast for metallographic examination of the surface detail.

The above replication technique offers a convenient and useful nondestructive method for "storing information" concerning the microstructural stages arising progressively during tensile testing, such as local yielding, twinning, carbide cracking, microcleavage, void formation, etc. On the other hand, this

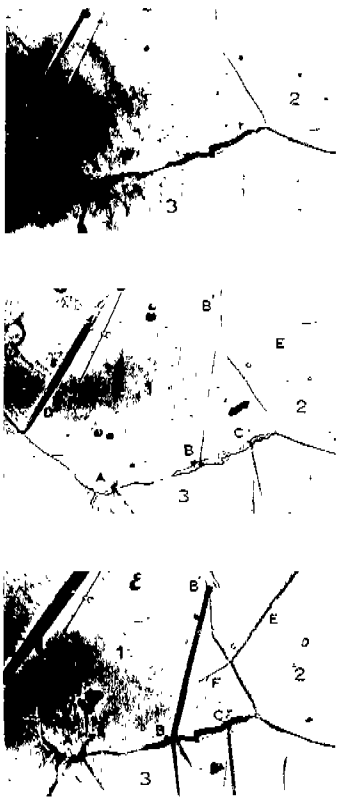

(a) Stressed to 66000 psi. Note crack in grain-boundary carbide at point A, initiating mechanical twins in grain 3.

(b) Stressed to 71000 psi. Cracks in the grain-boundary carbide have developed at points B and C, initiating twins in grain 3 and a cleavage microcrack (BB') in grain 1. Twin D in grain 1 has thickened, and a new twin E has formed in grain 2.

(c) Stressed to 76000 psi. Microcrack BB' in grain 1 has opened, causing localized plastic deformation in grain 2. Twins in grain 3 have widened. Widening of twin E in grain 2 has initiated twin F in grain 1.

Fig. 5. Sequence of Replica Photographs taken at three stages of loading of High - Purity Iron - 0.035% Carbon Alloy. Temperature of loading = -180°C. Tensile Axis Horizontal.

technique is limited to surface observations. For three-dimensional examination of these phenomena, sequential sectioning in one-mil increments was performed on some of the tensile specimens. In this way, many surface microcracks could be traced to their point of origin below the surface. Examples of replicas for a specimen of high-purity iron containing 0.035 percent carbon are shown in Figure 5.

It is found that, if carbide films are present along the ferrite grain boundaries, cracks appear in this brittle phase after some plastic deformation of the specimen, thus providing potent sites for the initiation of cleavage cracks in the adjacent grains of ferrite when the test temperature is sufficiently low or when the acting stresses are sufficiently high. This condition leads to the formation of microcleavage within or across a ferrite grain, and to cleavage failure when the propagation is able to continue across the grain boundaries.

It is possible that the differences in brittle-fracture behavior between furnace-cooled and air-cooled specimens may be traced to the presence of grain-boundary carbides in the furnace-cooled specimens. Some indication of this has already been observed. On comparing the tendency to form carbide films in the furnace-cooled steels, it is found that Steel E is the worst in this respect, Steel B is intermediate, and Steels BA and M exhibit the smallest propensity toward grain-boundary film formation. The furnace-cooled Steel C is about about equivalent to Steel BA on this basis, but air cooling significantly reduces the amount of grain-boundary carbide.

The observations on vacuum-melted iron demonstrate that small discrete carbides along the grain boundaries do not crack nearly as frequently as do continuous films, and the beneficial influence of manganese may be partially attributed to its action in promoting the formation of small globular carbides.

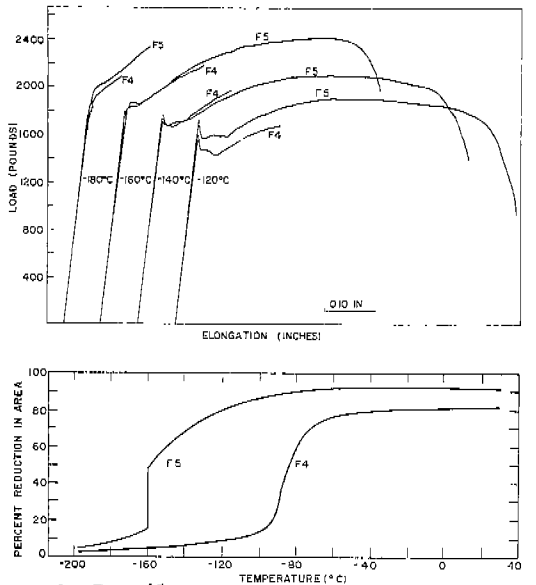

Fig. 6. Tensile-Test Data For Vacuum-Melted Iron Containing 0.035 Percent Carbon (F4) and 0.007 Percent Carbon (F5).

Manganese also refines the carbide lamellae in pearlite, which is a favorable effect because coarse carbides in pearlite can be susceptible to premature cracking during plastic deformation.

Systematic metallographic studies of vacuum-melted ferrites during tensile testing at temperatures between the ambient and -195° C showed that ferrite microcleavage cracks develop only after plastic flow sets in, and that they are initiated mainly by the cracking of carbides when the Griffith-Orowan condition is satisfied. The probability of ferrite cleavage increases with (a) decreasing test temperature, (b) increasing stress level, (c) amount of plastic strain, and (d) increasing thickness of the carbides being cracked. The latter cracks act as Griffith flaws. These factors cause the microcracking frequency to increase with decreasing temperature until the ease of crack propagation reduces the strain to fracture, and then fewer microcleavages are formed prior to failure. This accounts for the bell-shaped microcracking curve in Figure 1.

The remarkable differences in fracture characteristics between the two vacuum-melted ferrites respresented by the two families of load-elongation and ductility curves in Figure 6 are almost entirely due to differences in the amount and size of the carbides present[16]. Both polycrystalline materials have the same strain-hardening and twinning behavior, and yet the ductility-transition temperatures are quite dissimilar: T_d = -90° C for the iron with massive carbides (0.035 percent carbon) and -160° C for the iron with very few carbides (0.007 percent carbides).

Twin intersections and decohesion of twin/matrix interfaces are not significant sources of cleavage initiation in these specimens, but they can become more important (a) at test temperatures well below T_d, (b) in extremely coarse grain sizes and single crystals, (c) in the absence of grain-boundary carbides, and (d) in the presence of solution-hardening elements, like silicon and phosphorus, which raise the flow-stress level to the point where twinning can operate before the normal plastic yielding causes the carbides to crack.

It is well known that grain boundaries act as barriers to the propagation of cleavage cracks, and so most of the detected ferrite microcracks are of the order of one grain diameter in length. Consequently, a small grain size is more effective than a large grain size in inhibiting long-range propagation of cracks. In addition, the finer grain

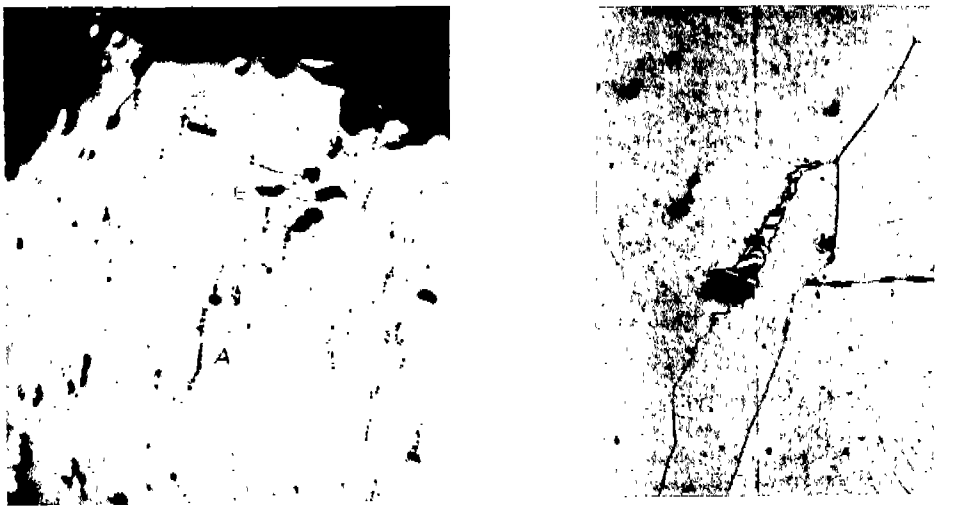

(a) 50× (b) 200×

Fig. 7. Initiation Of Voids Due To Carbide Cracking In Necked Region After Tensile Testing of Vacuum-Melted Iron (0.035 Percent Carbon) At -90° C. Reduction in Area = 32 Percent. Tensile Axis is Vertical.

size is more resistant to microcrack initiation because a given amount of intergranular carbide will then be spread over more grain-boundary area and will be correspondingly less massive. It will, therefore, produce smaller Griffith flaws upon cracking.

Cracked carbides also play a role in the ductile-fracturing process at temperatures above T_d. At the moment when a carbide crack reaches the carbide/ferrite interface, if the ferrite is able to deform plastically, the Griffith-Orowan condition will not be attained and a ferrite cleavage crack will not form. In this case, the carbide crack opens into a void, and eventually internal necking takes place between such voids, as depicted by the porosity in Figure 7. When these tiny necks break through, fibrous fracture ensues. The resulting ductility under these test conditions is relatively high, but it still varies inversely with the amount of massive carbide that undergoes cracking.

8. Cleavage Fracture in Iron Single Crystals

Flat single crystals of Puron iron (0.002 percent carbon, 0.001 percent nitrogen, 0.04 percent oxygen) and Ferrovac iron (0.001 percent carbon, 0.001 percent nitrogen, 0.003 percent oxygen) were prepared by the strain-anneal method, and tensile tested at subzero temperatures.[13]

Cleavage fracture is encountered below ~110° C in these ferrite crystals, and the initiation sites can be identified as (a) the interfaces at occluded (parasitic) grains, and (b) twin/twin intersections according to Figure 8. The latter circumstance consists of a moving twin striking an existing twin, often opening up one of the twin/matrix interfaces by local tensile stresses. Some examples are illustrated schematically in Figure 9. No cases were found of ferrite cleavage being initiated (a) by intersecting slip bands, (b) by two advancing twins coming together at their tips, or (c) by such twins emitting dislocations ahead along their intersecting paths. The rapid propagation of twins and their subsequent thickening are considered to be important factors in their ability to initiate cleavage when they are stopped by barriers such as pre-existing twins or occluded grains.

The presence of occluded grains in (otherwise) single crystals of iron is a common occurrence and, because the resulting interfaces are potential sites for cleavage initiation, this probably explains the wide scatter in fracture stress reported in the literature for iron crystals, even when crystallographic orientation is taken into account.

(a) 1000X

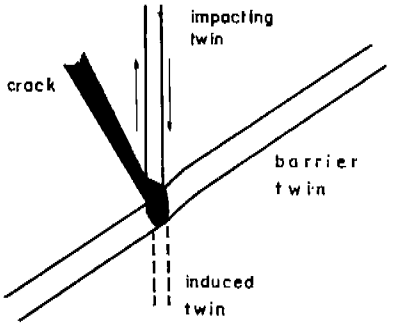

(b)

Fig. 8. Example Of Twin/Twin Intersection Mechanism Of Initiating Microcleavage. Vacuum Melted Iron (0.035 Percent Carbon) Tensile Tested At -150°C. (a) Actual Structure At 1000X; (b) Schematic Representation. Tensile Axis Is Horizontal. (Reduced 30% in reproduction)

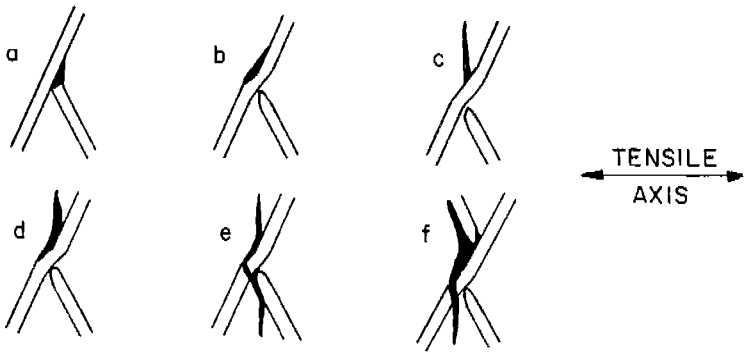

Fig. 9. Various Modes Of Microcleavage Initiation By Twin/Twin Intersection Mechanism.

Only a small fraction of the aforementioned interface cracks actually grow into cleavage cracks. Often the origin of the main cleavage crack can be located on the fracture surface by the direction of the cleavage steps or river markings. The most common type of cleavage source traced in this way is a twin/twin intersection in which the line of intersection lies in the {001} ferrite cleavage plane. When the line of twin intersection does not lie in a {001} plane of the ferrite, the local crack is less likely to switch to a cleavage crack, and correspondingly lower test temperatures (or higher operating stresses) are required for this type of cleavage initiation to become active.

It should be emphasized, however, that mechanical twinning loses its efficacy for cleavage initiation with increasing test temperature and decreasing grain size. Not only does the tendency toward twinning as a mode of deformation thereby decrease, but the ability of twin intersections to result in cleavage fracture also subsides because of the reduced rate of twin propagation and thickening. Thus, twinning ordinarily plays a minor role, if any, in causing or controlling the ductility-transition phenomena observed here in the polycrystalline iron and steel.

9. Twinning as a Means of Structural Refinement

The conditions under which twinning becomes important in inducing cleavage fracture have just been discussed in Section 8. There are instances, however, in which the twins produced by plastic deformation can interfere with the fracturing process. When microcracks form in the ferritic grains of polycrystalline iron and steel, they are frequently stopped by twins which come into existence during the prior deformation. In fact, such twins can provide barriers to cleavage propagation just as grain boundaries do. Some illustrative results are described below.

The properties of coarse-grained (0.30 - 0.40 mm) vacuum-melted iron (0.035 percent carbon) have been compared in the annealed condition and in the pretwinned condition (60 percent of the grains containing twins), the latter being achieved by 0.4 percent tensile strain at -195° C. This structural refinement lowers the ductility-transition temperature from -90° C to -135° C. On tensile testing at -120° C, the ductility of the annealed iron is about 7 percent reduction in area, whereas in the pretwinned condition the reduction in area increases to 70 percent. In another comparison, the coarse-grained vacuum-melted iron was pretwinned by 0.5 percent tensile strain at -160° C. Upon subsequent tensile testing at -110° C, the fracture stress is raised from 63,900 to 125,000 psi by the pretwinning, and the elongation to fracture is thereby increased from 16 to 39 percent. These improvements are actually greater than would be expected from an equivalent amount of grain refinement.

The above findings, based on the tensile testing of coarse-grained vacuum-melted iron, are due not only to an interference with crack propagation, but also to enhanced resistance to crack initiation. In pretwinned structures, the microcracks in the ferrite are fewer in number as well as shorter in length. The twin interfaces are somewhat mobile and furnish additional modes of local deformation that tend to relieve the microstresses which might otherwise satisfy the Griffith - Orowan criterion for cleavage initiation.

Unfortunately, these interesting phenomena are not readily applied to the practical problem of brittle fracture in mild steel. Pretwinning becomes more difficult to perform in the finer grain sizes encountered in mild steel, and the presence of pearlite also seems to inhibit mechanical twinning compared to very low-carbon iron. As a result, fewer twins per grain are produced in steels, even by rolling or shock loading at -195° C, than in the coarse-grained iron.

Furthermore, the pretwinning is not as beneficial in Charpy tests as in tensile tests. Possibly, in Charpy testing, not all the twins are effectively oriented to arrest cracks, compared to the previous case in which the twins are generated in tension and the testing is conducted in tension. It is also likely that the twin interfaces are not sufficiently mobile under high strain-rate conditions to relieve the microscale stresses which can initiate cleavage of the ferrite at carbide cracks. No significant lowering of the 15 ft - lb Charpy transition temperature of the mild steels with normal grain size was achieved by the pretwinning treatments.

10. Micromechanisms of Fracture in the Presence of Notches

10.1 Notched Tensile Tests

Because the cracking of intergranular carbides can provide fracture sources at relatively low stresses (Section 7), this phenomenon can be used to good advantage in sorting out the various mechanisms and sequences of fracture. Under such circumstances, fracture can be started (and located) at stresses which are not high enough to cause long-range propagation. This is particularly appropiate when

the initiation processes are localized, as in the presence of notches. The vacuum-melted iron with 0.035 percent carbon is an excellent material for this purpose. The following description of the fracturing stages is based on a ferritic grain size of 0.10 - 0.15 mm (ASTM No. 4-3) and edge-notched flat tensile specimens with a 19/16 X 0.304 X 0.120 inch gage section.

Table II shows how the ductility-transition temperature is influenced by the notch geometry (with the notch radius being held constant at 0.010 inch as in the case of Charpy specimens). T_d depends on the notch depth, but is insensitive to the notch angle.

A family of load-elongation curves for these notched tensile specimens is given in Figure 10 as a function of test temperature. The overall trends in strength and ductility with decreasing temperature are regular, but an anomalous double yield point appears below room temperature down to about -90° C. This behavior, arising because of the notches, is not unique with the vacuum-melted iron under discussion; it is also observed in mild steels. The enlarged load-elongation curve in Figure 11 and the accompanying schematic insert help elucidate the double-yielding process. Gross yielding in stage 2 (drop in load from A to B) occurs along two arcs or plastic hinges between the notches, thus encompassing what will be termed the "notched volume." Gross yielding spreads throughout the notched volume by Lüders deformation at essentially constant load in stage 3. Strain hardening from B to C then takes place in the notched volume during stage 4, until gross yielding starts in the outer volume (stage 5). Lüders deformation in the outer volume proceeds at constant load in stage 6, after which strain hardening ensues during stage 7. At or near point D, where the load is commensurate with that previously sustained by the notched volume, the deformation is taken up again by the notched volume because of the higher stress there (stage 8). Eventually, if the temperature is high enough, necking across the notched volume sets in and the load drops once more until rupture takes place.

The ultimate fracture occurs in the notched volume, as discussed in detail below, and the extent to which the several deformation stages are revealed depends on when the fracturing sets in. As the testing temperature is lowered, the above stages are successively cut off by the entree of fracture at earlier points. The temperature below which the necking is interceded by fracture is the ductility-transition temperature (T_d), just as in the case of unnotched tensile specimens.

The micromechanisms of the fracturing process will now be described for specimens having a notch depth of 0.030 inch and a T_d of about -75° C (Table II).

At temperatures above -60° C, carbides undergo cracking in the notched volume during the initial gross yielding (stage 2, Figure 11), and because the ferrite is able to deform locally, voids open up during the subsequent stages 3 and 4. These voids in the notched volume then remain unchanged while the outer volume takes up the plastic flow in stages 5, 6 and 7, but they continue to grow in size and number when plastic flow is resumed in the notched volume during stage 8. Carbide cracking and void formation occur in the outer volume, concommitant with the deformation there, but the main action leading to the ultimate fracture takes place in the notched volume because of the higher stresses due to the reduced section.

The actual rupture path follows an arc along one of the two original plastic hinges between the notches (Figure 12) and the prior necking also follows the same curved path. On a microscale, this path is the locus of local necking between the voids formed at cracked carbides (Figure 13), and the resulting fracture is fibrous. The gross rupture starts at the notches when the local necking between a void and the notch tip breaks through; an example is shown in Figure 14.

In the vicinity of the transition temperature, approximately - 60 to -80°, there are two modes of fracture in these notched tensile specimens: the fibrous rupture just described and cleavage, both being initiated mainly by the cracking of carbides. Thus, when the carbides crack, competition exists as to whether the adjacent ferrite will flow plastically to generate a void, or whether the ferrite will undergo microcleavage. The lower the test temperature, the more the latter process is favored over the former. At any given temperature in this range, the first microcleavage cracks are located about 1 mm (or about 5 - 10 grain diameters) away from the root of the notch. Evidently, this is the critical point where (a) plastic flow causes cracking of the carbides at an early stage, and (b) the attendant tensile stress is high enough due to the nearby notch to satisfy the local Griffith-Orowan condition for cleaving the ferrite. Other microcleavages then come into existence elsewhere in the notched volume as the loading is increased.

Figure 15 illustrates how the microcleavage frequency in the notched volume relates to the load-elongation curve. These

TABLE. II. DUCTILITY-TRANSITION TEMPERATURE OF DOUBLY NOTCHED TENSILE SPECIMENS OF VACUUM-MELTED IRON WITH 0.035% CARBON.

Grain Size = 0.10-0.15 mm (ASTM No. 4-3)

Notched Depth (in.)	Ratio to Gage Section*	Notch Angle	T_d (°C)
0	0	180°	-110
0.030	0.198	90°	- 75
0.030	0.198	45°	- 75
0.030	0.198	0°	- 70
0.047	0.310	90°	- 35

* *Includes Both Notches.*

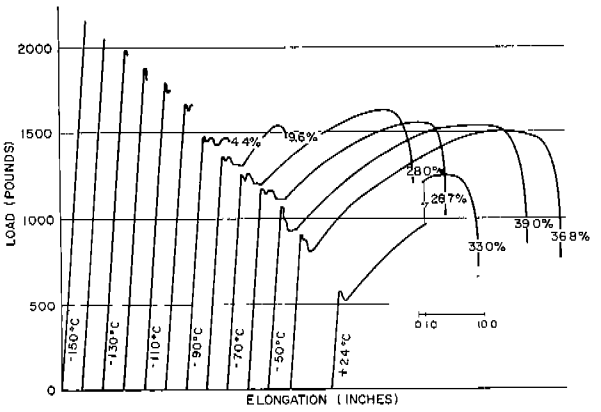

Fig. 10. Tensile Curves For Notched Specimens Of Vacuum - Melted Iron (0.035 Percent Carbon).

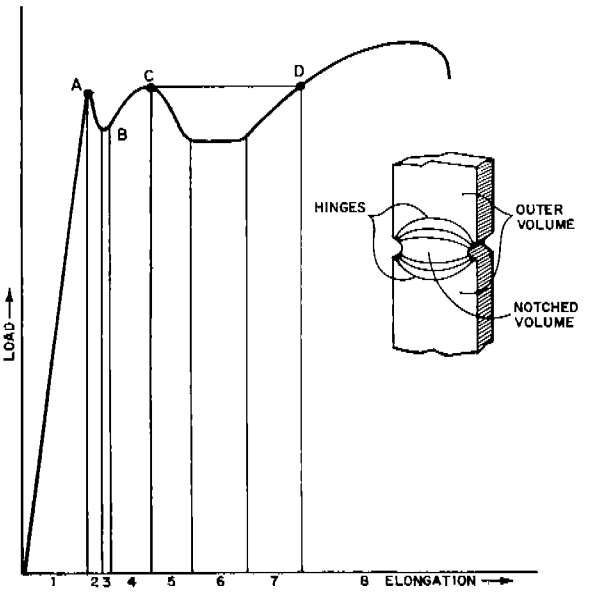

Fig. 11. Typical Load-Elongation Curve For Notched Specimen Of Vacuum-Melted Iron (0.035 Percent Carbon) Tensile Tested At About -90°C.

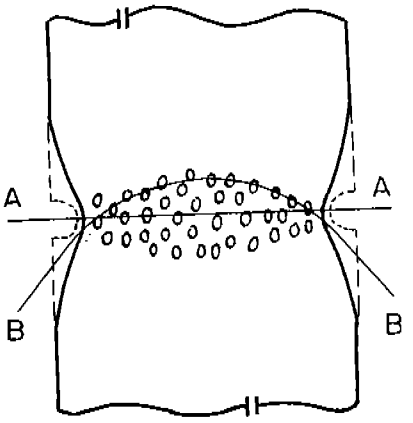

Fig. 12. Schematic Illustration Of Fibrous Rupture Along ARC Between Notches.

Fig. 14. Fibrous Rupture About To Start Due To Connecting - Up Of Voids With Notch Root.

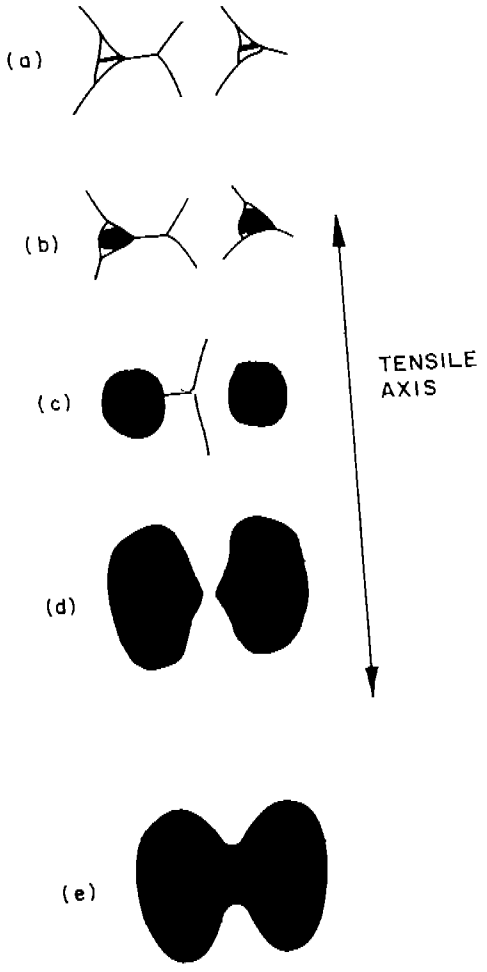

Fig. 13. Sequence Of Carbide Cracking, Void Formation And Growth, Local Necking Between Voids, And Connecting - Up Of Voids.

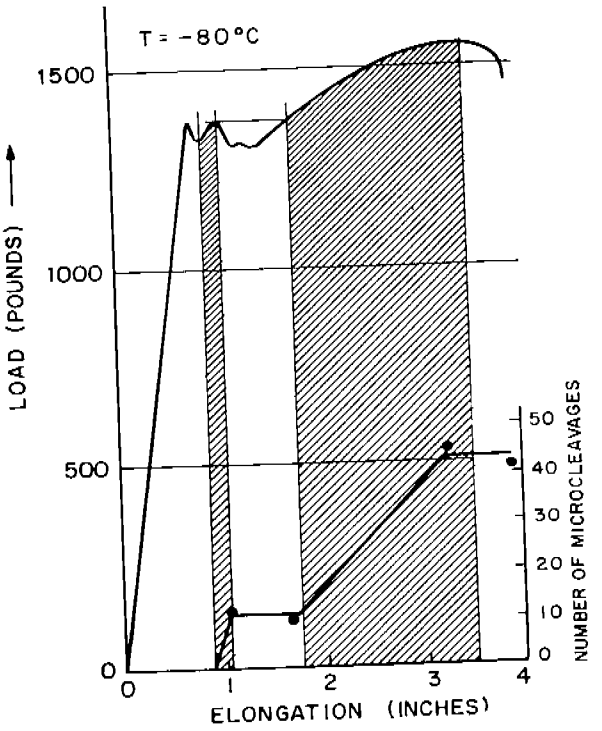

Fig. 15. Load-Elongation Curve For Vacuum-Melted Iron (0.035 Percent Carbon) Showing Number Of Microcleavages In Notched Volume During Tensile Testing At -80°C.

cracks occur primarily during the strain-hardening of the notched volume, corresponding to stages 4 and 8 in Figure 11, but not, of course, during the strain hardening of the outer volume. The main fracture starts when the bridge between the early microcracks and the notch roots breaks through, in this instance by local necking. If general necking has occurred before then, the fracture will tend to follow an arc between the notches, as in the high temperature range, but will consist of a mixture of ductile tearing and cleavage facets. With progressive lowering of the test temperature, the fracture becomes more cleavage, intercepts the necking process, and the path of fracture straightens out between the notches. In the latter event, additional carbide cracking and microcleavage take place ahead of the advancing fracture. In this temperature range, the new cleavages together with some of the existing ones connect up with the main crack by (a) tearing, (b) shearing, or (c) local necking.

We now consider the micromechanisms of fracture in the notched tensile specimen at temperatures below T_d. Between -80 and -110° C, general yielding and some strain hardening take place in the notched volume before fracture, and the path lies directly across between the notches. Although the macro-fracture is entirely cleavage, there is substantial prior deformation at the notches, and microcleavages are generated first at the critical point near (not at) the notch root. The main fracture starts when the intervening bridge breaks through to the notch, but unlike the higher-temperature situation, this break-through results from secondary cleavage. Moreover, as the main crack then advances across the notched volume, the linking up of microcracks with the ultimate fracture is taken over by secondary cleavage through the intervening bridges. Under these conditions, the ductility is rather low, but it is finite because gross yielding in the notched volume has ensued prior to failure.

On tensile testing the notched specimens between -120 and -130° C, only the beginning of gross yielding is detected prior to fracture, and the reduction in area is only about 0.5 percent. Very few, if any, microcleavage cracks in the ferrite are found, although the main fracture is entirely cleavage. It is inferred that, in line with the observations at somewhat higher temperatures, local plastic deformation occurs first at the notches, carbides crack there, and the operating stress is high enough, not only to initiate cleavage, but to keep it propagating to failure. Under these conditions, the advancing cleavage can move across grain boundaries even without producing microcracks just ahead. There is no problem about this when the adjacent ferrite grains have almost the same crystallographic orientation, but even when they are quite misaligned (as they are in general), the main cleavage can traverse grain boundaries by splitting into segments of cleavage on the new {100} planes, with cleavage steps in-between such that the overall orientation of the fracture in the second grain is the same as that in the first grain. This type of compatibility of the cleavage process between grains is indicated in Figure 16. It requires a high stress for operation because of the energy associated with the cleavage steps. Hence, while the grain boundaries ordinarily act as good barriers to the propagation of cleavage, they are by no means insurmountable barriers.

At -140° C and below, no general yielding is detected before fracture, and the resulting reduction in area is practically nil. Here, the mode of deformation is essentially by mechanical twinning, and now the cleavage fracture is initiated by twin/twin intersections, as described in Section 8. An example is shown in Figure 8. In addition, such twin intersections can occasionally be identified as the source of cleavage on the fracture surface. The cleavage-propagation process is especially complex and unpredictable. Not only do the grain boundaries act as barriers which, however, can be penetrated by the cleavage-splitting mechanism in Figure 16, but pre-existing twins also provide barriers. However, these barriers can be surmounted as illustrated in Figure 17. The running crack can emit a mechanical twin which, in turn, collides with an existing twin and a new cleavage is thereby initiated. The latter becomes incorporated into the main crack by secondary cleavage.

Accordingly, mechanical twinning can control both the initiation and propagation of cleavage fracture, but in the notched tensile specimens under study, these phenomena operate only at temperatures well below T_d.

10.2 Notched-Bend Tests

The microdetails of fracture in the presence of notches were also studied in three-point slow bending, using regular V-notch Charpy specimens of the above vacuum-melted ferrite with 0.035 percent carbon. The prior treatment consisted of a four-hour anneal at 1250° C, followed by furnace cooling, and resulting in a ferritic grain size of 0.225 - 0.295 mm (ASTM No. 2-1). Three-dimensional metallography was carried out by successive sectioning in from the side faces of the specimens after loading to various stages along the load-deflection curves, and also after

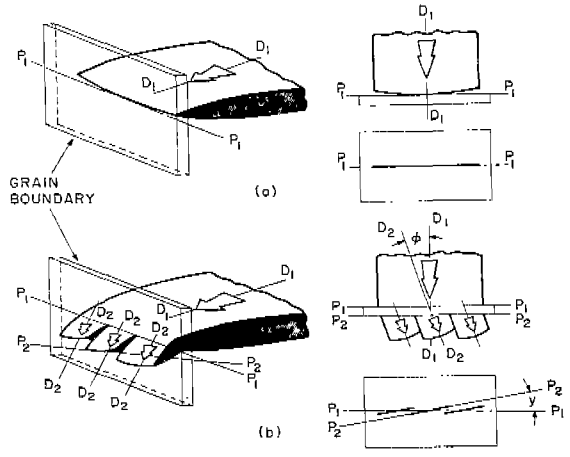

Fig. 16. Propagation Of Microcleavage Across A Grain Boundary With (a) Cleavage Direction And Plane In Grain 1 Parallel To Grain 2, And (b) Cleavage Direction And Plane In Grain 1 Nonparallel To Grain 2.

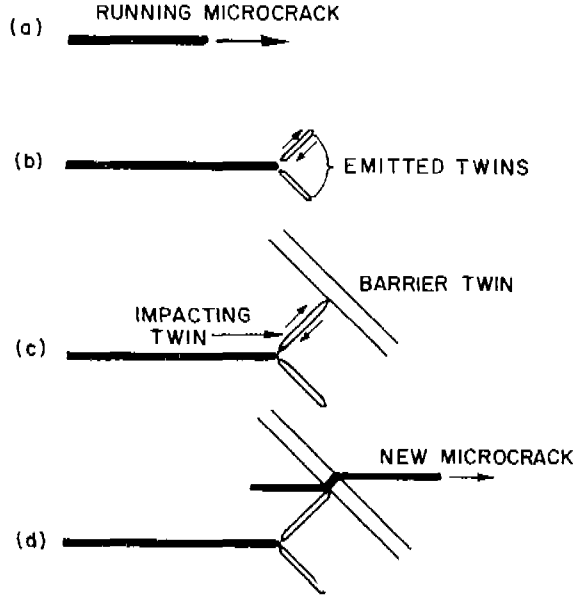

Fig. 17. Mode Of Microcleavage Re-Initiation Through An Existing Twin Barrier.

complete fracture. In this way, the prevailing micromechanisms could be ascertained during the course of testing as a function of temperature.

A family of load-deflection curves for these tests is shown in Figure 18. There are three characteristic temperature ranges, as denoted in Figure 19. In range I, above -45^{0} C, gross yielding occurs by slip and spreads across the notched section of the specimen before fracture, leading to considerable ductility. In range II, between -45^{0} and -90^{0} C, fracture sets in during general yielding, and the corresponding ductility is low (but not zero). Mechanical twinning follows the onset of yielding and becomes more pronounced with decreasing test temperature in this range. Below -90^{0} C, in range III, twinning supersedes slip as the primary mode of deformation, and fracture takes place without gross yielding across the specimen. The ductility is then virtually nil, although significant local deformation can be detected at the root of the notch.

The ductility-transition temperature in these notched slow-bend tests is -45^{0} C, and is taken as the temperature below which fracture sets in along with, or prior to, general yielding. In principle, this criterion for the transition temperature is different from that employed for the tensile tests, the latter being the temperature below which fracture sets in prior to the necking instability. However, the necking stage does not arise in the notched-bend test, and the criterion adopted here becomes a more realistic index. All of the drop-in-load exhibited by the curves in Figure 18 is due to the progressive advance of the fracturing process across the bend specimen.

At all temperatures where gross yielding occurs, carbide cracking is encountered, and these cracks provide the sites for voids or microcleavage depending on the temperature and local stress conditions. In the upper part of range I, the final rupture is entirely fibrous, and starts via local necking between the voids at the root of the notch at the side faces of the specimen. This separation process then spreads across the section as indicated in Figure 20A. In the lower part of range I, however, where the fracture stress is decreasing, cleavage initiation and propagation begin to compete with the fibrous rupturing. Microcracks lying about one millimeter (4-5 grain diameters in this case) below the notch break through the root along the length of the notch, as depicted in Figure 20B, and then long-range cleavage ensues. This consists of the repeated initiation of microcracks and their linking up with the main cleavage by localized tearing

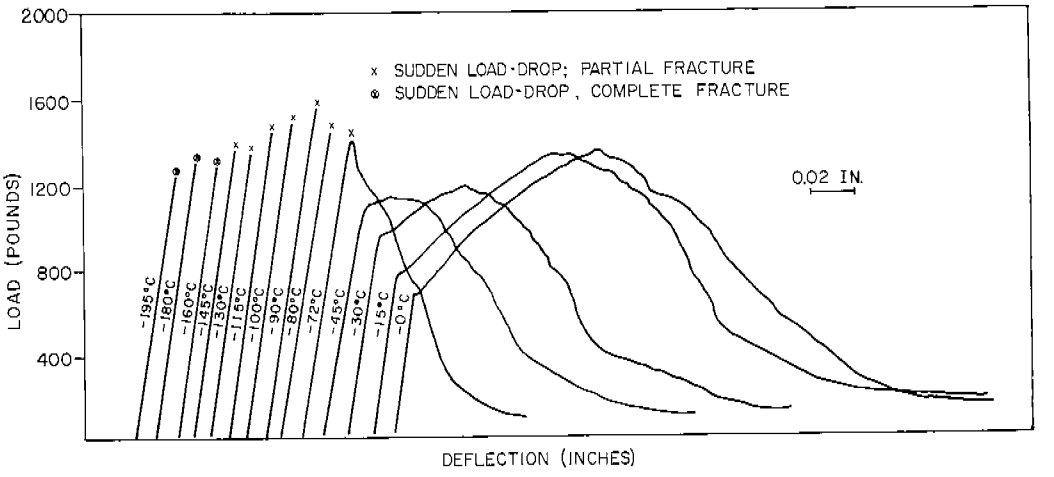

Fig. 18. Load-Deflection Curves For Notched Slow-Bend Specimens Of Iron - 0.035 Percent Carbon As Traced From Autographic Recorder.

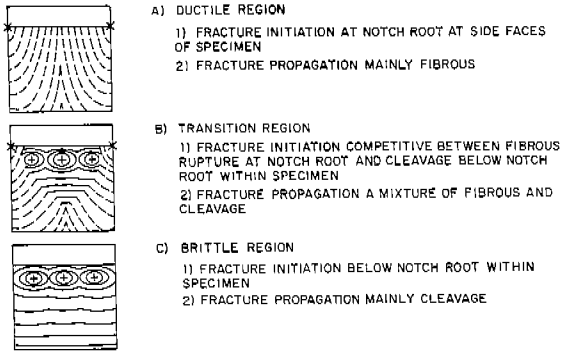

Fig. 20. Schematic Illustration Of Initiation And Subsequent Propagation Of Fracture In Notched Slow-Bend Specimens Of Iron - 0.035 Per Cent Carbon.

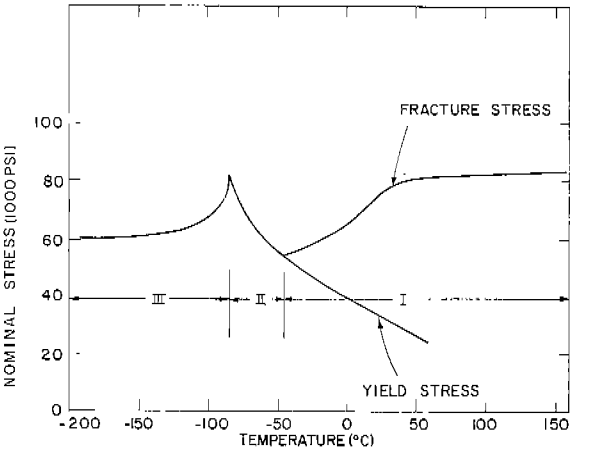

Fig. 19. Slow-Bend Properties Of Iron - 0.035 Per Cent Carbon.

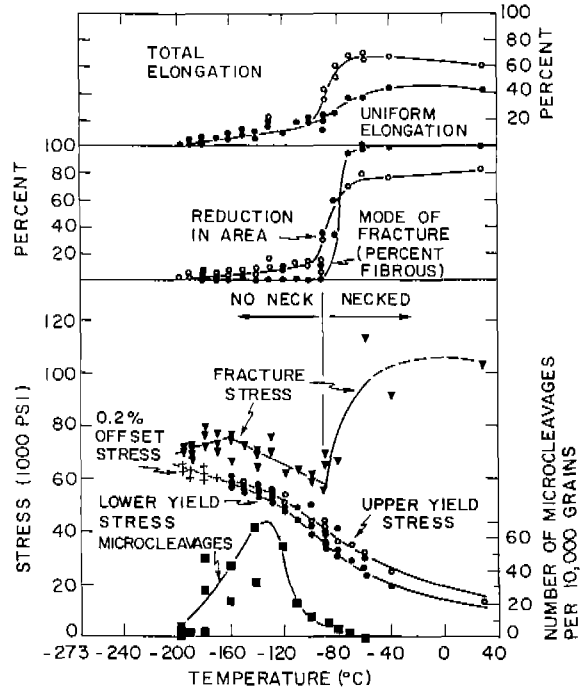

Fig. 21. Tensile Properties Of Vacuum-Melted Iron (0.035 Percent Carbon); 0.30 To 0.40 mm Grain Size.

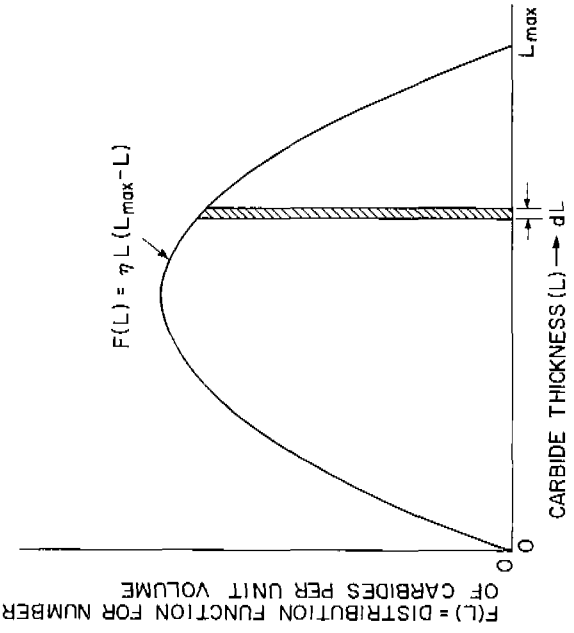

Fig. 22. Assumed Parabolic Distribution Of Carbide Thicknesses Ranging From L_{max} Down To Zero.

of the intervening material. In this way, the main cleavage crack advances along the length of the notch and into the specimen section, to occupy a fraction of the final fracture surface that increases with decreasing temperature. Mixtures of fibrous and cleavage fracture straddle the transition temperature; actually, cleavage does not extend across the entire section until the lower end of range II. In range III, the fracture is entirely cleavage, and again initiates from microcracks forming in the interior of the specimen about one millimeter below the notch root (Figure 20C). Here, however, twinning is the principal mode of deformation, as noted before, and twin intersections with other twins and with grain boundaries become an important source of cleavage initiation, competing with the carbide-cracking mechanism that predominates at higher temperatures. On the other hand, pre-existing twins can also act as microcrack arrestors as described more fully in section 9.

The above phenomena are entirely consistent with those observed in the tensile test, but the various sequences of deformation and fracture are modified with respect to the degree of overlap and temperature ranges because of the different states of stress. These manifestations are also found in mild steels, but the various stages are not as readily sorted out because the carbide-cracking "indicators" are then more difficult to discern. The subject vacuum-melted iron magnifies these effects and permits a more exact description of the fracturing process.

11. Statistical Nature of Cleavage Initiation

We now return to the tensile testing of smooth-bar specimens in order to present a more quantitative treatment of cleavage initiation as a statistical event. Again it is advantageous to use the vacuum-melted polycrystalline iron (with 0.035 percent carbon) as an illustrative material. The tensile data are summarized in Figure 21.

It is assumed that, when a carbide cracks and thereby produces a Griffith flaw of length L, the adjacent ferrite will undergo microcleavage if the tensile stress σ_t on a family of potential cleavage planes satisfies the Griffith-Orowan relationship:

$$\sigma_t \geq \left[\frac{2E\,\gamma_{eff}}{\pi\,(1-\nu^2)L}\right]^{1/2} \qquad (1)$$

where: E = Young's modulus

γ_{eff} = effective surface energy (including energy expended in plastic straining)

ν = Poisson's ratio

γ_{eff} is the order of 5,000 ergs/cm^2 in the temperature range where microcleavages are first observed[17], and $\left[\frac{2 E \gamma_{eff}}{\pi (1 - \nu 2)}\right]^{\frac{1}{2}}$ then equal 7 X 10^{15} c.g.s. units for the material under consideration. L is taken to be the full length of the carbide crack (rather than one-half its length, as is usually done for internal cracks) because this type of Griffith flaw produces microcleavage in a given ferritic grain like an edge crack on a microscale. Ocassional microcleavages are often detected in tensile-tested specimens at temperatures well above the ductility-transition temperature, but they begin to appear in rapidly increasing numbers as the test temperature approaches T_d (-90^0 C in the case at hand), and reach a maximum somewhat below T_d (Figure 21). This bell-shaped trend has been discussed previously in Section 7. Below a certain temperature, no microcleavages are found, in that the conditions for initiating a microcrack likewise satisfy the conditions for long-range propagation to failure.

There will be a distribution of carbide thicknesses in the specimen which will range from L_{max} down to zero. For simplicity, we assume a parabolic distribution function.

$$F(L) = \eta L (L_{max} - L) \qquad (2)$$

where F(L) dL is the number of carbides per unit volume having thicknesses between L and L + dL. This relationship is shown in Figure 22. The normalizing factor η is determined by the total number of carbides* per unit volume N_V and the area under the curve in Figure 22:

$$N_V = \int_0^{L_{max}} F(L)\, dL, \text{ or}$$

$$\eta = \frac{N_V}{\int_0^{L_{max}} L (L_{max} - L)\, dL} = 6\, N_V / L^3_{max} \qquad (3)$$

Other things being equal, L_{max} is proportional to the carbon content, and is also proportional to the grain diameter because most of the relevant carbides are spread out along the grain boundaries.

The carbides crack during straining of the ferrite (undoubtedly because of bending of the carbides), and we assume that the number N_V^+ of such cracks per unit volume is proportional to the plastic strain ε_p. This will give a distribution of carbide-crack thicknesses ranging up to L_{max} for each ε_p, but the total number of such cracks in the distribution will increase with the plastic straining, as indicated schematically in Figure 23 for four positions along the stress-strain curve. At each such point, microcleavage will result only from those carbide cracks whose length L is large enough to satisfy equation (1) at the accompanying stress level.

As we move from one carbide crack-length distribution to the next with increasing plastic strain in Figure 23, the acting stress also increases, and carbide cracks of smaller and smaller length are able to initiate microcleavage of the ferrite by satisfying equation (1). The L values corresponding to the four stress levels (respresents by the four distribution curves) in Figure 23 are given along the horizontal axis. At stress σ_1, which might be the yield stress, this illustrative example indicates that the critical Griffith-flaw length $L(\sigma_1)$ is larger than L_{max}, and hence microcleavage does not occur at this level of stress (and strain). At some higher stress σ_2, the critical flaw length is then down to $L(\sigma_2)$, which is below L_{max}, and so microcleavage can take place. The number of microcleavages per unit volume (N_V^m) thus generated up to (σ_2,ε_2) is given by area A, and is equal to the number of supercritical carbide cracks in the carbide crack-length distribution at strain ε_2, minus all those in the same size range that formed previously at lower strains but were then subcritical because the stress was too low. The latter carbide cracks are considered to remain inactive at stress σ_2 because of blunting. This is in line with the fact that, ordinarily, carbide cracks either initiate microcleavage at their instant of formation (if they are supercritical) or not at all.

As the tensile loading is further raised, say to (σ_3, ε_3) and then to (σ_4, ε_4), areas

---

* We are concerned only with the massive carbides which, upon cracking, can initiate microcleavage of the ferrite.

A + B and A + B + C denote the corresponding number of microcleavages per unit volume (N_v^m) generated by the carbide-cracking process. Of course, this is actually a progressive, rather than a stepwise phenomenon, and for each successive level of (σ,ε), there is a distribution of carbide-crack lengths (N_v^+ vs. L) due to the strain ε, and a minimum value of L that just satisfies the Griffith-Orowan condition for microcleaving the ferrite at the existing stress σ. The latter relationship forms the lower boundary of the shaded areas in Figure 23, thus defining the number of microcleavage events per unit volume (N_v^m) occurring up to any point (σ, ε) along the stress-strain curve under the assumptions at hand.

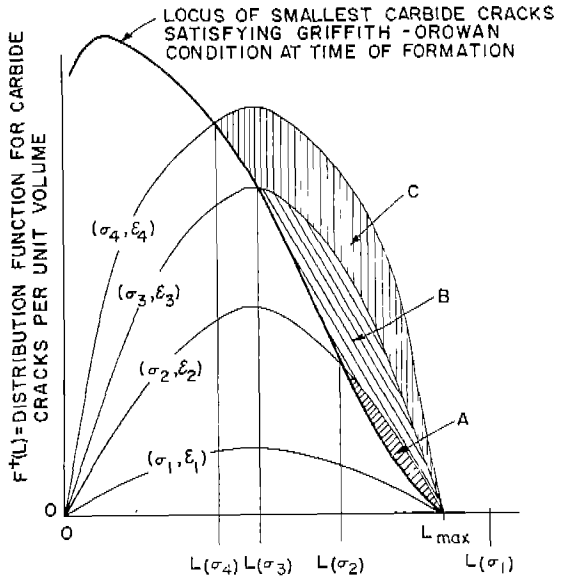

Fig. 23. Distribution of Carbide-Crack Lengths For Various Positions (σ,ε) Along The Stress - Strain Curve. Shaded Areas Signify Number of Carbide Cracks Satisfying Griffith-Orowan Condition At Time Of Formation.

AREA A Number of Micro-Cleavages Formed Up To (σ_2, ε_2).

AREA B Number of Micro-Cleavages Formed Between (σ_2,ε_2) And (σ_3,ε_3).

AREA C Number of Micro-Cleavages Formed Between (σ_3,ε_3) And (σ_4,ε_4).

It is now possible to calculate N_v^m up to the point of fracture, knowing the stress-strain curve and the number of carbide cracks (N_v^+) that form as a function of plastic strain. If we assume that

$$N_v^+ = K\, N_V\, \varepsilon_p, \text{ then} \qquad (4)$$

$$F^+(L) = KF(L)\varepsilon_p \text{ and } N_v^+ = \int F^+(L)\, dL = K \int \varepsilon_p\, F(L)dL \qquad (5)$$

Thus, up to the point of fracture:

$$N_v^m = K\varepsilon_f \int_{L(\sigma_f)}^{L_{max}} F(L)dL - K\int_{L(\sigma_f)}^{L_o} \varepsilon_p\, F(L)dL \qquad (6)$$

$$= K\varepsilon_f \int_{L(\sigma_f)}^{L_{max}} \eta L\,(L_{max} - L)dL - K\int_{L(\sigma_f)}^{L_o} \varepsilon_p\, \eta L(L_{max} - L)dL \qquad (7)$$

$$= 6\left(\frac{KN_V}{L^3_{max}}\right) \left\{ \varepsilon_f \int_{L(\sigma_f)}^{L_{max}} L(L_{max} - L)dL - \int_{L(\sigma_f)}^{L_o} \varepsilon_p\, L(L_{max} - L) \right\} dL \qquad (8)$$

where σ_f and ε_f = fracture stress and strain respectively.

$L_o = L_{max}$ for $L(\sigma_y) > L_{max}$ (this is the case shown in Figure 23)

$L_o = L(\sigma_y)$ for $L(\sigma_y) < L_{max}$ (this is the case when some of the carbide cracks forming at σ_y are immediately supercritical)

σ_y = yield stress (where $\varepsilon_p > 0$ and carbides begin to crack)

ε_f is taken as the uniform strain up to the point of fracture because the available quantitative measurements on microcleaving have been made in the uniform portion of the gage length.

As a first step, we allow KN_v/L^3_{max} to be an adjustable parameter in order to show the form of the N_v^m vs. T curve. Equation (8) can then be solved graphically for each stress-strain curve (at each temperature), and the results are summarized in Figure 24. Here it is evident that the calculated curve successfully matches the bell shape of the experimental curve. A KN_v/L^3_{max} value of $10^{13}cm^{-6}$ gives the best fit for this vacuum-melted iron, and checks within a factor of 2 with that obtained from the measured values of K, N_v and L_{max}.

In the vacuum-melted iron under discussion, most of the carbon is in the form of intergranular carbides, and the metallographic parameters N_v and L_{max} in equation (8) change accordingly with carbon content and grain size. The effect of these variables are indicated in Figures 25 and 26, where comparisons are drawn between the observed and calculated microcleavage frequencies. Again, the statistical model accounts for observed trends.

It has been found that, when carbide cracks forming at the yield stress happen to be of sufficient size to initiate micro-cleavage at that stress, there is then a good chance that complete fracture will occur before the necking stress is reached. Hence, as an approximation, we shall now assume that T_d can be identified with the temperature at which L_{max} satisfies the Griffith-Orowan condition at the yield stress (lower yield stress if discontinuous yielding occurs). In Figure 23, this criterion for T_d amounts to finding the temperature where $L(\sigma_1) = L(\sigma_y) = L_{max}$. The transition temperatures calculated on this basis are compared with the experimental ductility-transition temperatures in Table III for a series of iron-carbon alloys in various conditions. The extent of agreement is much better than justified, but again points up the importance of carbide cracking as a source of cleavage fracture in these materials.

Another striking test is given in Table IV in which the ductility and necking behavior of four presumably identical specimens exhibit substantial scatter at T_d, as is often noted. For the two specimens that fractured before necking, their parameters show that $L(\sigma_y) < L_{max}$ which means that the condition for microcleavage was satisfied at the yield stress, whereas for the other two specimens which necked, $L(\sigma_y) > L_{max}$. Thus, relatively small differences in the yield strength and the carbide size can lead to major differences in ductility, merely by controlling whether or not necking sets in before fracture.

It should be emphasized, however, that this treatment of the fracture-initiation process cannot be expected to remain valid for those materials, steels or otherwise, in which the carbide-cracking phenomenon is either absent or superseded by other fracture sources.

12. Macrocrack Formation

It is very difficult to extrapolate the micromechanisms of fracture to the large-scale failure of constructional shapes. The remaining problem is to bridge the gap between fracturing processes at the micro-level and macrocracks that reach inches or feet in length.[17] Here is the place where metallographic phenomena and continuum fracture mechanics must be brought together; however, that important step lies outside the mainstream of the present program.

The initiation of microcleavage cracking has already been discussed in considerable detail, and methods by which such cracks can join others or traverse grain boundaries have also been described. More attention should now be focussed on the microscopic sequences that lead to unstable macrocracks. The crack-extension force for microcleavage initiation is about $\gamma = 5000$ ergs/cm^2 [17]; in this case, a grain of ferrite is presented with an extremely sharp notch, say from a carbide that is cracking. Under the conditions which satisfy equation (1), microcleavage starts in an unstable fashion, but it can soon be arrested at a barrier. In order for this microcrack to traverse the barrier or to link up with another crack by breaking-through the intervening bridge of metal, a much larger crack-extension force is necessary, corresponding to the plane-strain G_{Ic} values determined in large-scale notched-plate tests. For the class of materials studied here, G_{Ic} falls in the range of 3-15 X 10^6 ergs/cm^2, indicating that macrocrack propagation through polycrystalline material is a vastly more difficult process than microcrack propagation across a grain.[17] At least part of this remarkable difference

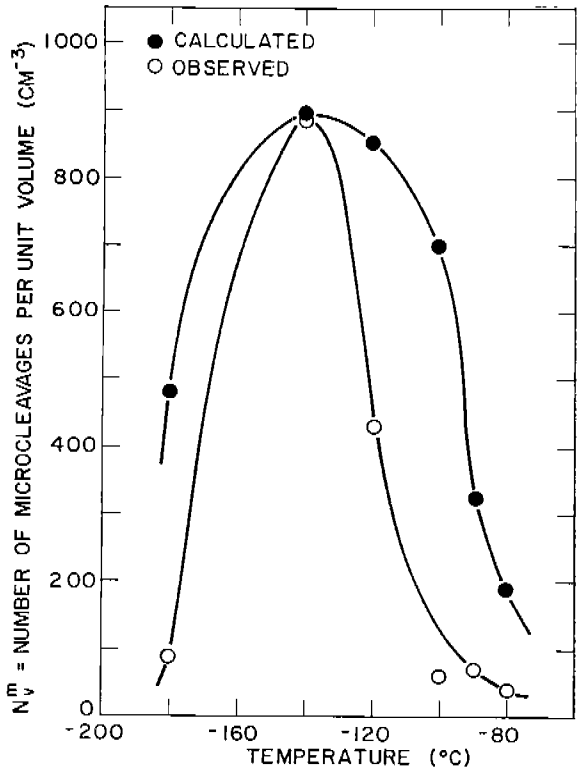

Fig. 24. Comparison Of Calculated And Observed Microcleavage Frequency In Tensile - Tested Specimens Of Vacuum-Melted Iron (0.035 Percent Carbon); Curves Matched At -140°C.

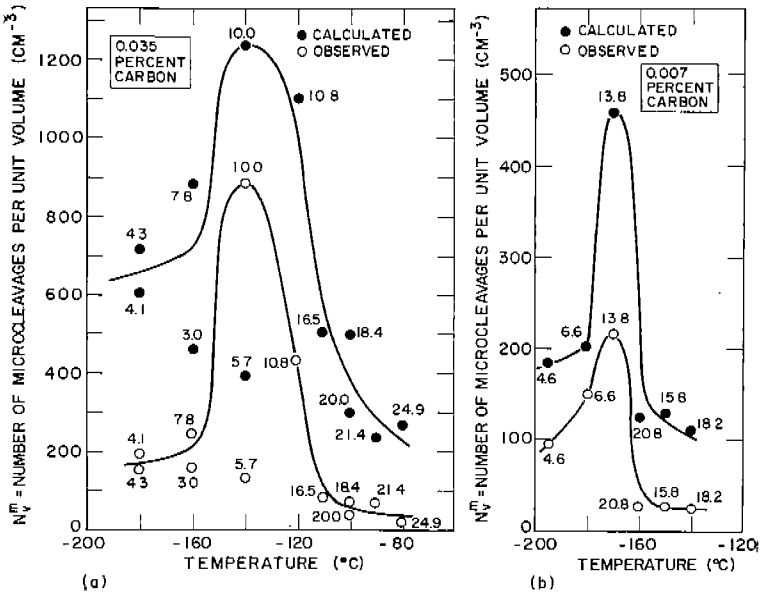

Fig. 25. Effect Of Carbon Content On Calculated And Observed Number Of Microcleavages In Tensile-Tested Vacuum-Melted Iron With (a) 0.035 Percent Carbon, (b) 0.007 Percent Carbon; Grain Diameter = 0.25 To 0.35 MM. Numbers Indicate Percent Uniform Elongation To Fracture.

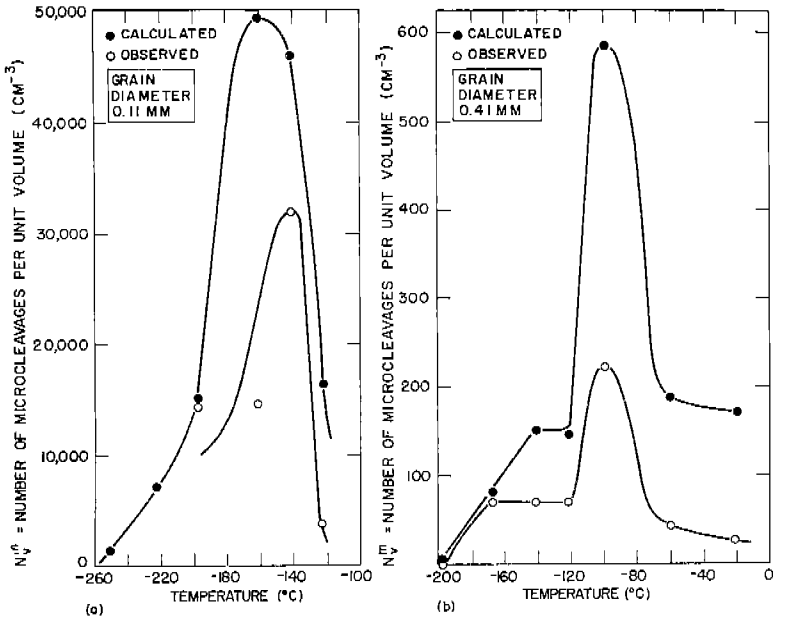

Fig. 26. Effect Of Grain Size On Calculated And Observed Number Of Microcleavages In Tensile-Tested Vacuum-Melted Iron (0.039 Percent Carbon) With (a) Grain Diameter = 0.11 MM, And (b) Grain Diameter = 0.41 MM.

TABLE III. DUCTILITY-TRANSITION TEMPERATURES OF A SERIES OF VACUUM-MELTED IRON-CARBON ALLOYS, AS MEASURED IN TENSILE TESTS AND CALCULATED ACCORDING TO THE STATISTICAL CARBIDE-CRACKING MODEL.

w/o C	Grain Size (mm)	Condition	$L_{max}(\mu)$	T_d (°C) Observed	T_d (°C) Calculated
0.007	0.24	Annealed	3.7	-170	-165
0.018	0.11	Recrystallized	2.0	-190	-190
	0.14	Recrystallized	2.6	-140	-170
0.035	0.15	Annealed	5.3	-110	-110
	0.34	Annealed	12.0	- 90	- 90
	0.32	WQ from 705°C	5.5	- 90	- 80
0.039	0.11	Annealed	4.3	-130	-120
	0.40	Annealed	15.8	- 50	- 50

TABLE IV. ELUCIDATION OF SCATTER IN DUCTILITY AND NECKING BEHAVIOR ON TENSILE TESTING AT T_d = -90° C. VACUUM-MELTED IRON WITH 0.035% CARBON.

Grain Size (mm)	σ_y dy/cm^2	Necking	% Reduction in Area	$L(\sigma_y)$ (μ)	L_{max} (μ)	Comparisons
0.34	2.42×10^9	No	7.9	12.0	12.0	$L(\sigma_y) = L_{max}$
0.34	2.45×10^9	No	13.6	11.7	12.0	$L(\sigma_y) < L_{max}$
0.30	2.34×10^9	Yes	31.3	12.8	10.6	$L(\sigma_y) > L_{max}$
0.31	2.47×10^9	Yes	32.3	11.5	11.0	$L(\sigma_y) > L_{max}$

may result from the substantial plastic zone that precedes the advance of a large crack, even in the absence of gross yielding. On the other hand, large amounts of elastic energy can be stored in heavy sections, and become available to drive the crack if gross yielding is inhibited.

The basic material parameters that control the macrocrack-extension force and the conditions under which a macrocrack will start, run and stop have yet to be examined in the same metallurgical detail as the microfracturing processes elucidated in this program.

Acknowledgments

The participants in this research program warmly appreciate the long-range sponsorship of the Ship Structure Committee as well as the sustained technical guidance of the Committee on Ship Steel and the Ship Hull Research Committee. The Committee members most directly concerned with this work were Professor John Chipman, Dr. M. W. Lightner, Dr. John R. Low, Jr., and Professor Charles S. Barrett. Professor Barrett also chaired a Project Advisory Committee comprised of Dr. James H. Bechtold, Dr. L. S. Darken and Professor Maxwell Gensamer.

Special credit is due to staff members of the National Academy of Sciences who were associated with the contractual part of this project: Dr. David K. Felbeck, Mr. Arthur R. Lytle, and Mr. Richard W. Rumke.

Throughout the program at M.I.T., Mr. R. C. Whittemore, Miss Miriam Yoffa and Mr. E. D. Howell furnished splendid assistance in the testing and metallographic phases of the research, and provided much of the continuity in the "coming and going" of graduate students. Miss Marguerite Meyer also played a most valuable role in the administration of this project over the years.

References

1. C. S. Barrett and W. E. Mahin, "A Review of Ship Steel Research and Recommendations for Future Studies," SSC-70 (15 February 1954).

2. Fracture, edited by B. L. Averbach, D. K. Felbeck, G. T. Hahn, and D. A. Thomas, John Wiley and Sons (1959).

3. Proc. First International Conference on Fracture, edited by T. Yokobori, T. Kawasaki and J. L. Swedlow, Japanese Society for Strength and Fracture of Materials (1966).

4. W. S. Owen, B. L. Averbach and Morris Cohen, "The Tensile Yield Behavior of Ship Steel," Ship Structure Committee Report SSC-103, (September 28, 1956).

5. W. S. Owen, D. H. Whitmore, Morris Cohen and B. L. Averbach, "The Relation of Charpy Impact Properties to the Microstructure of Three Ship Steels, " The Welding Journal Research Supplement (November 1957)36 503s.

6. W. S. Owen, M. Cohen and B. L. Averbach, "Some Aspects of Preyield Phenomena in Mild Steel at Low Temperatures," Trans. ASM (1958) 50 517.

7. W. S. Owen, B. L. Averbach and M. Cohen, "Brittle Fracture of Mild Steel in Tension at -196^{0} C," Trans. ASM (1958) 50 634.

8. W. S. Owen, Morris Cohen and B. L. Averbach, "The Influence of Ferrite Banding on the Impact Properties of Mild Steel," The Welding Journal Supplement (August 1958) 368.

9. G. T. Hahn, W. S. Owen, B. L. Averbach and M. Cohen, "Micromechanism of Brittle Fracture in a Low-Carbon Steel," The Welding Journal Research Supplement (September 1959) 38 367s.

10. G. T. Hahn, B. L. Averbach, W. S. Owen and Morris Cohen, "Initiation of Cleavage Microcracks in Polycrystalline Iron and Steel," Fracture, John Wiley and Sons (1959).

11. B. L. Averbach, "Brittle Fracture," J. Eng. Mech. Div., Proc. Am. Soc. Civil Eng. (1960) 86 No. EM6, 29.

12. G. T. Hahn, Morris Cohen and B. L. Averbach, "The Yield and Fracture Behavior of Mild Steel with Special Reference to Manganese," JISI (August 1962) 200 634.

13. W. F. Flanagan, B. L. Averbach and M. Cohen, "Effect of Substructure on Cleavage in Iron Crystals," SSC-133 (29 January 1962).

14. A. R. Rosenfield, B. L. Averbach and Morris Cohen, "Twinning Occurrence in Iron Single Crystals," Acta Met. (1963) 11 No. 9, 591.

15. C. J. McMahon, Jr., "Micromechanisms of Cleavage Fracture in Polycrystalline Iron," Ship Structure Committee Report SSC-161 (1964).

16. C. J. McMahon, Jr. and Morris Cohen, "Initiation of Cleavage in Polycrystalline Iron, "Acta Met. (June 1965) 13 No. 6,591.

17. B. L. Averbach, "Micro-and Macrocrack Formation, "Ship Structure Report SSC-171 (1965); Proc. First International Conference on Fracture (1965) 2 779.

18. C. J. McMahon, Jr. and Morris Cohen, "The Fracture of Polycrystalline Iron," Proc. First International Conference on Fracture (1965) 2 779.

19. B. L. Averbach, "Some Physical Aspects of Fracture," to be published.

NONE

Security Classification

DOCUMENT CONTROL DATA - R&D

(Security classification of title, body of abstract and indexing annotation must be entered when the overall report is classified)

1. ORIGINATING ACTIVITY *(Corporate author)*: Massachusetts Institute of Technology

2a. REPORT SECURITY CLASSIFICATION: none

2b. GROUP: ------

3. REPORT TITLE: Metallurgical Structure and the Brittle Behavior of Steel

4. DESCRIPTIVE NOTES *(Type of report and inclusive dates)*: 1954 - 1966

5. AUTHOR(S) *(Last name, first name, initial)*: Cohen, Morris

6. REPORT DATE: May 1968

7a. TOTAL NO. OF PAGES: 24

7b. NO. OF REFS: 19

8a. CONTRACT OR GRANT NO.: NObs 88229

b. PROJECT NO.: SR - 136

c.

d.

9a. ORIGINATOR'S REPORT NUMBER(S): none

9b. OTHER REPORT NO(S) *(Any other numbers that may be assigned this report)*: SSC - 183

10. AVAILABILITY/LIMITATION NOTICES: Qualified requesters may obtain copies of this report from DDC

11. SUPPLEMENTARY NOTES: This was a Ship Structure Committee Project.

12. SPONSORING MILITARY ACTIVITY: Naval Ship Systems Command

13. ABSTRACT

By means of surface-replication and three-dimensional metallography, it has become possible to delineate the interrelated processes of slip, twinning, carbide cracking, void formation and microcleavage in the tensile testing of iron and mild steels at subatmospheric temperatures.

Mechanical twinning plays a complex but secondary role in these polycrystalline materials. On the other hand, pre-existing twins can act as barriers to the propagation of cleavage fracture, thereby leading to a lowering of T_d and enhanced ductility. These beneficial effects of pre-existing twins are quite pronounced in tensile tests, but they are less advantageous in Charpy testing.

The cracking of intergranular carbides is an especially potent means of microcleavage initiation, and can be used as a "tell-tale" to follow the fracturing sequences. There are indications that the amount and size of intergranular carbides in mild steels are reduced by decreased carbon content, increased manganese content, increased cooling rate from the austenitizing temperature, and decreased grain size.

The initiation of microcleavage via carbide cracking can be treated statistically, on the assumption that the number of carbide cracks per unit volume is proportional to the plastic strain, and that the size distribution of carbide cracks at any given strain is parabolic up to the maximum size present.

An important step remains to connect up these microfracturing processes with macrocrack formation in plate sections.

DD FORM 1 JAN 64 1473

NONE

Security Classification

NONE

Security Classification

14. KEY WORDS	LINK A		LINK B		LINK C	
	ROLE	WT	ROLE	WT	ROLE	WT

INSTRUCTIONS

1. ORIGINATING ACTIVITY: Enter the name and address of the contractor, subcontractor, grantee, Department of Defense activity or other organization *(corporate author)* issuing the report.

2a. REPORT SECURITY CLASSIFICATION: Enter the overall security classification of the report. Indicate whether "Restricted Data" is included. Marking is to be in accordance with appropriate security regulations.

2b. GROUP: Automatic downgrading is specified in DoD Directive 5200.10 and Armed Forces Industrial Manual. Enter the group number. Also, when applicable, show that optional markings have been used for Group 3 and Group 4 as authorized.

3. REPORT TITLE: Enter the complete report title in all capital letters. Titles in all cases should be unclassified. If a meaningful title cannot be selected without classification, show title classification in all capitals in parenthesis immediately following the title.

4. DESCRIPTIVE NOTES: If appropriate, enter the type of report, e.g., interim, progress, summary, annual, or final. Give the inclusive dates when a specific reporting period is covered.

5. AUTHOR(S): Enter the name(s) of author(s) as shown on or in the report. Enter last name, first name, middle initial. If military, show rank and branch of service. The name of the principal author is an absolute minimum requirement.

6. REPORT DATE: Enter the date of the report as day, month, year; or month, year. If more than one date appears on the report, use date of publication.

7a. TOTAL NUMBER OF PAGES: The total page count should follow normal pagination procedures, i.e., enter the number of pages containing information.

7b. NUMBER OF REFERENCES: Enter the total number of references cited in the report.

8a. CONTRACT OR GRANT NUMBER: If appropriate, enter the applicable number of the contract or grant under which the report was written.

8b, 8c, & 8d. PROJECT NUMBER: Enter the appropriate military department identification, such as project number, subproject number, system numbers, task number, etc.

9a. ORIGINATOR'S REPORT NUMBER(S): Enter the official report number by which the document will be identified and controlled by the originating activity. This number must be unique to this report.

9b. OTHER REPORT NUMBER(S): If the report has been assigned any other report numbers *(either by the originator or by the sponsor)*, also enter this number(s).

10. AVAILABILITY/LIMITATION NOTICES: Enter any limitations on further dissemination of the report, other than those imposed by security classification, using standard statements such as:

(1) "Qualified requesters may obtain copies of this report from DDC."

(2) "Foreign announcement and dissemination of this report by DDC is not authorized."

(3) "U. S. Government agencies may obtain copies of this report directly from DDC. Other qualified DDC users shall request through _____."

(4) "U. S. military agencies may obtain copies of this report directly from DDC. Other qualified users shall request through _____."

(5) "All distribution of this report is controlled. Qualified DDC users shall request through _____."

If the report has been furnished to the Office of Technical Services, Department of Commerce, for sale to the public, indicate this fact and enter the price, if known.

11. SUPPLEMENTARY NOTES: Use for additional explanatory notes.

12. SPONSORING MILITARY ACTIVITY: Enter the name of the departmental project office or laboratory sponsoring *(paying for)* the research and development. Include address.

13. ABSTRACT: Enter an abstract giving a brief and factual summary of the document indicative of the report, even though it may also appear elsewhere in the body of the technical report. If additional space is required, a continuation sheet shall be attached.

It is highly desirable that the abstract of classified reports be unclassified. Each paragraph of the abstract shall end with an indication of the military security classification of the information in the paragraph, represented as *(TS), (S), (C), or (U)*.

There is no limitation on the length of the abstract. However, the suggested length is from 150 to 225 words.

14. KEY WORDS: Key words are technically meaningful terms or short phrases that characterize a report and may be used as index entries for cataloging the report. Key words must be selected so that no security classification is required. Identifiers, such as equipment model designation, trade name, military project code name, geographic location, may be used as key words but will be followed by an indication of technical context. The assignment of links, roles, and weights is optional.

NONE

Security Classification

NATIONAL ACADEMY OF SCIENCES-NATIONAL RESEARCH COUNCIL

DIVISION OF ENGINEERING

The Ship Research Committee undertakes research service activities in the general fields of materials, design, and fabrication, as relating to improved ship hull structure, when such activities are accepted by the Academy as part of its functions. The Committee recommends research objectives and projects; provides liaison and technical guidance to such studies; reviews project reports; and stimulates productive avenues of research.

SHIP RESEARCH COMMITTEE

Chairman: Mr. M. L. Sellers, (I, II, III)
Naval Architect
Newport News Shipbuilding and Drydock Co.

Vice Chairman: Dr. J. M. Frankland (I, II, III)
(Retired) Mechanics Division
National Bureau of Standards

Members

Mr. William H. Buckley (I, II)
Chief, Structural Criteria
Bell Aerosystems Co.

Mr. B. B. Burbank (III)
(Retired) Chief Metallurgist
and Chemist
Bath Iron Works Corp.

Dr. D. P. Clausing (III)
Fundamental Research Laboratory
U. S. Steel Research Center

Mr. Donald P. Courtsal (II, III)
Dravo Corp.
Engineering Works Division

Mr. A. E. Cox (I, II)
Assistant Naval Architect
Newport News Shipbuilding
and Drydock Co.

Professor J. E. Goldberg (I, II)
School of Civil Engineering
Purdue University

Dr. N. H. Jasper (I)
Technical Director
U.S. Navy Mine Defense Laboratory

Mr. W. R. Jensen (I, II)
Structural Methods Engineer
Grumman Aircraft Engineering Corp.

Mr. G. E. Kampschaefer, Jr. (III)
Manager, Application Engineering
ARMCO Steel Corp.

Professor Bryan R. Noton (II, III)
Visiting Professor
Dept. of Aeronautics and Astronautics
Stanford University

Dr. Stanley T. Rolfe (III)
U. S. Steel Corp.
Applied Research Center

Mr. Merville Willis (I)
General Manager
Ship Design Division
Consultec, Inc.

Professor R. A. Yagle (II)
Professor, Marine Engineering
University of Michigan

(I) - *Advisory Group I, Ship Strain Measurement & Analysis*
(II) - *Advisory Group II, Ship Structural Design*
(III) - *Advisory Group III, Metallurgical Studies*

A. R. Lytle
Director

R. W. Rumke
Executive Secretary

SHIP STRUCTURE COMMITTEE PUBLICATIONS

These documents are distributed by the Clearinghouse, Springfield, Va. 22151. These documents have been announced in the Technical Abstract Bulletin (TAB) of the Defense Documentation Center (DDC), Cameron Station, Alexandria, Va. 22314, under the indicated AD numbers. There is no charge for documents for registered users of the DDC services. Other users must pay the prescribed rate set by the Clearinghouse.

Index of Ship Structure Committee Publications (1946 - April 1965)

SSC-170, *Studies of Some Brittle Fracture Concepts* by R. N. Wright, W. J. Hall, S. W. Terry, W. J. Nordell and G. R. Erhard. September 1965. AD 473496.

SSC-171, *Micro - and Macrocrack Formation* by B. L. Averbach. October 1965. AD 473496.

SSC-172, *Crack Extension and Propagation Under Plane Stress* by A. R. Rosenfield, P. K. Dai and G. T. Hahn. March 1966. AD 480619.

SSC-173, *Exhaustion of Ductility Under Notch Constraint Following Uniform Prestraining* by C. Mylonas, S. Kobayashi and A. Armenakas. August 1966. AD 637143.

SSC-174, *Investigation of Residual Stresses in Steel Weldments* by K. Masubuchi and D. C. Martin. September 1966. AD 639619.

SSC-175, *Mechanical Properties of a High-Manganese, Low-Carbon Steel for Welded Heavy-Section Ship Plate* by R. D. Stout and C. R. Roper, Jr. August 1966. AD 637211.

SSC-176, *Biennial Report of the Ship Structure Committee*. June 1966. AD 641333.

SSC-177, *Guide for Interpretation of Non-Destructive Tests of Welds in Ship Hull Structures* by The Weld Flaw Evaluation Committee. September 1966. AD 639053.

SSC-178, *A Survey of Some Recent British Work on the Behaviour of Warship Structures* by J. Clarkson. November 1966. AD 644738.

SSC-179, *Residual Strains and Displacements within the Plastic Zone Ahead of A Crack* by J. Cammett, A. R. Rosenfield, and G. T. Hahn. November 1966. AD 644815.

SSC-180, *Experimental Determination of Plastic Constraint Ahead of a Sharp Crack Under Plane-Strain Conditions* by G. T. Hahn and A. R. Rosenfield. December 1966. AD 646034.

SSC-181, *Results from Full-Scale Measurements of Midship Bending Stresses on Two Dry-Cargo Ships- Report #2* by D. J. Fritch, F. C. Bailey, J. W. Wheaton. March 1967. AD 650239.

SSC-182, *Twenty Years of Research Under the Ship Structure Committee* by S. R. Heller, Jr., R. Nielsen, Jr., A. R. Lytle, John Vasta. December 1967. AD 663677.